



Crustal structure of the northwestern Basin and Range Province and its transition to unextended volcanic plateaus

D. W. Lerch

Department of Geological and Environmental Sciences, Stanford University, Building 320, Stanford, California 94305, USA

Department of Geophysics, Stanford University, Mitchell Building 353, Stanford, California 94305, USA

Now at Environmental Studies, Feather River College, 570 Golden Eagle Avenue, Quincy, California 95971, USA (dlerch@frc.edu)

S. L. Klemperer

Department of Geophysics, Stanford University, Mitchell Building 353, Stanford, California 94305, USA

J. M. G. Glen and D. A. Ponce

U.S. Geological Survey, MS 989, 345 Middlefield Road, Menlo Park, California 94025, USA

E. L. Miller

Department of Geological and Environmental Sciences, Stanford University, Building 320, Stanford, California 94305, USA

J. P. Colgan

U.S. Geological Survey, MS 989, 345 Middlefield Road, Menlo Park, California 94025, USA

[1] The northwestern margin of the Basin and Range Province is characterized by a transition from low-magnitude (~20%) extension in northwestern Nevada to relatively unextended volcanic plateaus in northeastern California. Seismic-velocity and potential-field modeling provides new control on the Mesozoic-to-present tectonic evolution of this poorly understood portion of the U.S. Cordillera. We document ~20% crustal thinning associated with Basin and Range extension from a crustal thickness of ~37 km under northeastern California to ~31 km under northwestern Nevada that is consistent with the amount of extension recorded in the upper crust in northwestern Nevada, suggesting the crustal response to extension was relatively homogeneous over the entire crustal column. Our modeling also shows a well-defined, 80-km-wide zone of unusually low upper-crustal velocities (~5.9–6.1 km/s) that coincide with the surface location of sparse Cretaceous granites, locating the elusive northern extension of the Sierra Nevada batholith through northwestern Nevada for the first time in the subsurface. Combining geological and geophysical data, we reconstruct the late Cretaceous-to-present crustal evolution of this region, documenting an interplay between magmatic addition to the crust, erosional exhumation, sedimentation, and extension that has reversed the direction of crustal thinning from a west-facing continental margin to an east-facing interior basin margin over this time interval. Finally, we find no evidence in northwestern Nevada for unusually thick crust (>40 km) prior to Basin and Range extension.

Components: 3868 words, 12 figures, 1 table.

Keywords: Basin and Range; crustal seismology; gravity; transition zone; tectonics.

Index Terms: 1299 Geodesy and Gravity: General or miscellaneous (1709); 7205 Seismology: Continental crust (1219); 8109 Tectonophysics: Continental tectonics: extensional (0905).

Received 24 July 2006; **Revised** 30 October 2006; **Accepted** 20 November 2006; **Published** 23 February 2007.

Lerch, D. W., S. L. Klemperer, J. M. G. Glen, D. A. Ponce, E. L. Miller, and J. P. Colgan (2007), Crustal structure of the northwestern Basin and Range Province and its transition to unextended volcanic plateaus, *Geochem. Geophys. Geosyst.*, 8, Q02011, doi:10.1029/2006GC001429.

1. Introduction

[2] Despite extensive research over the last ~100 years in the northern Basin and Range Province (Figure 1) [e.g., *Emmons*, 1907], its northwestern margin remains little-studied. This region is characterized by a transition from Basin and Range extension in northwestern Nevada to high volcanic plateaus in northwesternmost Nevada, northeastern California, and southern Oregon. Geologic and thermochronologic studies document a later (≤ 12 Ma), lower magnitude ($\leq 20\%$) extensional history in northwestern Nevada [e.g., *Colgan et al.*, 2004, 2006a] than in the central portion of the northern Basin and Range (≤ 30 Ma and 50–100%) [e.g., *Gans et al.*, 1989; *Best and Christiansen*, 1991; *Smith et al.*, 1991; *Christiansen et al.*, 1992]. Despite minor upper-crustal extension across the northwestern margin of the Basin and Range, previous nearby geophysical surveys (COCORP 40°N and 1986 PASSCAL surveys) suggested that crustal thicknesses in this region (~30–32 km) are as thin or thinner than the more highly extended region to the south (~30–36 km, Figure 1) [e.g., *Klemperer et al.*, 1986; *Catchings and Mooney*, 1991]. West of this transition zone, Moho depth increases to 38–40 km beneath the Modoc Plateau in northern California (Figure 1) [e.g., *Zucca et al.*, 1986; *Mooney and Weaver*, 1989]. Because no data exists across this transition zone between the unextended lava plateaus and the northwestern Basin and Range, the details of how the change in crustal thickness is accomplished are unknown.

[3] Two likely explanations for the phenomenon of thin crust in a region of low upper-crustal extension are (1) that the crust in the northwestern corner of the Basin and Range was simply not as thick as that of central Nevada to begin with or (2) that strain has been heterogeneous with depth, allowing for significant lower-crustal thinning with only minor upper-crustal extension. Resolution of this question has important implications for the nature of how extensional deformation

takes place in continental crust. In the central portion of the northern Basin and Range, differential strain between the upper and lower crust is thought to maintain homogeneous crustal thicknesses despite local variations in upper-crustal extension [e.g., *Gans*, 1988]. On what length scales can lower-crustal deformation decouple from upper-crustal deformation? If the northwestern margin of the Basin and Range possessed pre-extensional crustal thicknesses comparable to central Nevada (perhaps as much as ~45–50 km [e.g., *Smith et al.*, 1991]), then long-wavelength lower-crustal flow would have been necessary to produce the modern Moho depths.

[4] To address the apparent discrepancy between the magnitude of upper-crustal extension in the northwestern Basin and Range with respect to its suspected thin crust, we collected a ~300 km seismic refraction/reflection/teleseismic profile and a ~260 km potential field profile across this portion of the Basin and Range, spanning the transition to the unfaulted crust of the Modoc Plateau (Figures 1 and 2). Our data document ~20% crustal thinning associated with Basin and Range extension and are consistent with the low-magnitude extension ($\leq 25\%$) recorded at the surface, suggesting that extensional strain has been approximately homogeneous with depth across this portion of the Basin and Range. In addition, we observe no evidence in our survey area for the distributed lower-crustal reflectivity commonly attributed to large-magnitude ductile strain in the central portion of the Basin and Range [e.g., *Catchings*, 1992]. Utilizing our data to reconstruct the evolution of the northwestern Basin and Range, we step backward through time, estimating the relative importance of various tectonic and magmatic events from Late Cretaceous to the present. Our simple reconstruction offers a significantly different image of crustal structure at ~90 Ma, when the crustal thickness of the western end of our survey area was less than the eastern end, opposite to its present-day configuration, and the thickest crust was only equal to the global conti-

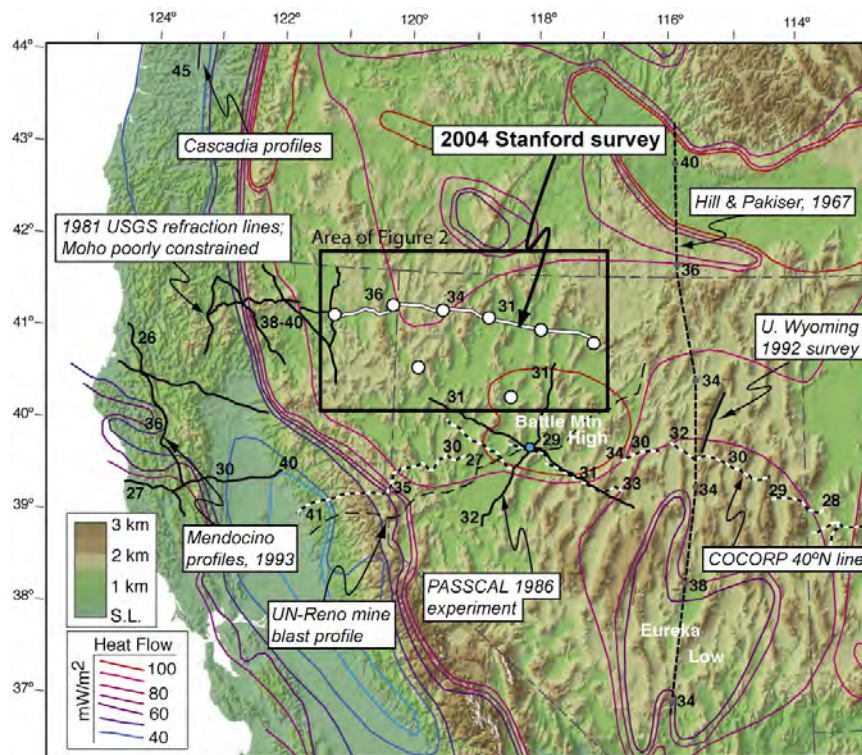


Figure 1. Map summarizing topography, heat flow [Blackwell et al., 1991], and relevant seismic data in the northern Basin and Range Province. Dashed black and white lines indicate COCORP seismic reflection profiles [Allmendinger et al., 1987]; solid black lines indicate PASSCAL experiment [Catchings and Mooney, 1991], Wyoming Ruby profile [Stoerzel and Smithson, 1998], USGS profiles in northern CA [Zucca et al., 1986], Cascadia profiles [Trehu et al., 1994], and Mendocino profiles from Beaudoin et al. [1996]. Short dashed black line shows profile of Hill and Pakiser [1976]; long dashed black line shows mine-blast profile of the University of Nevada, Reno [Louie et al., 2004]. Small blue circle near the intersection of the 1986 PASSCAL lines: their Shotpoint 4, described in text. Our 2004 experiment shown by white line (seismographs) and circles (shotpoints). Numbers along seismic lines indicate crustal thickness in kilometers.

mental average (~ 41 km [Christensen and Mooney, 1995]).

2. Regional Geology and Geophysics

[5] The northwestern margin of the Basin and Range is characterized by limited exposures of all but the most recent volcanic units because it is affected by only a minor amount of surface faulting. East of the Sheldon Plateau (Figure 2), Paleozoic and Mesozoic sedimentary and volcanic rocks (described in more detail below) form the most deeply exhumed footwall portions of the tilted fault blocks. West of and including the Sheldon Plateau, no pre-Tertiary exposures are present along our transect, and the only Paleogene units are found in the Warner Range tilt block. Despite the seeming paucity of geologic constraints across this region, we have derived a constrained tectonic history that is consistent with both the geophysical and geological data.

2.1. Pre-40 Ma: East of the Black Rock Range

[6] The eastern portion of the northwestern Basin and Range contains Paleozoic and Mesozoic rock units that record multiple episodes of convergence, and consist of highly deformed Cambrian-Mississippian basinal sequences of the Roberts Mountain allochthon, the Pennsylvanian-Permian sediments of the Antler Overlap Assemblage, and allochthonous upper Paleozoic deep-water sediments and Permian arc sequences of the Golconda allochthon [e.g., Stewart and Carlson, 1978; Miller et al., 1992; Wyld, 1992]. This late Paleozoic convergent history was followed by Triassic-early Jurassic extension, when thick (~ 6 km) siliciclastic and carbonate sedimentary sequences accumulated in a subsiding basin [Wyld, 2000]. Plutons that form the eastern part of the Sierra Nevada batholith intrude these rock units, and range in age from 196 to 102 Ma [Quinn et al., 1997]. In their regional study and synthesis of Mesozoic contact metamor-

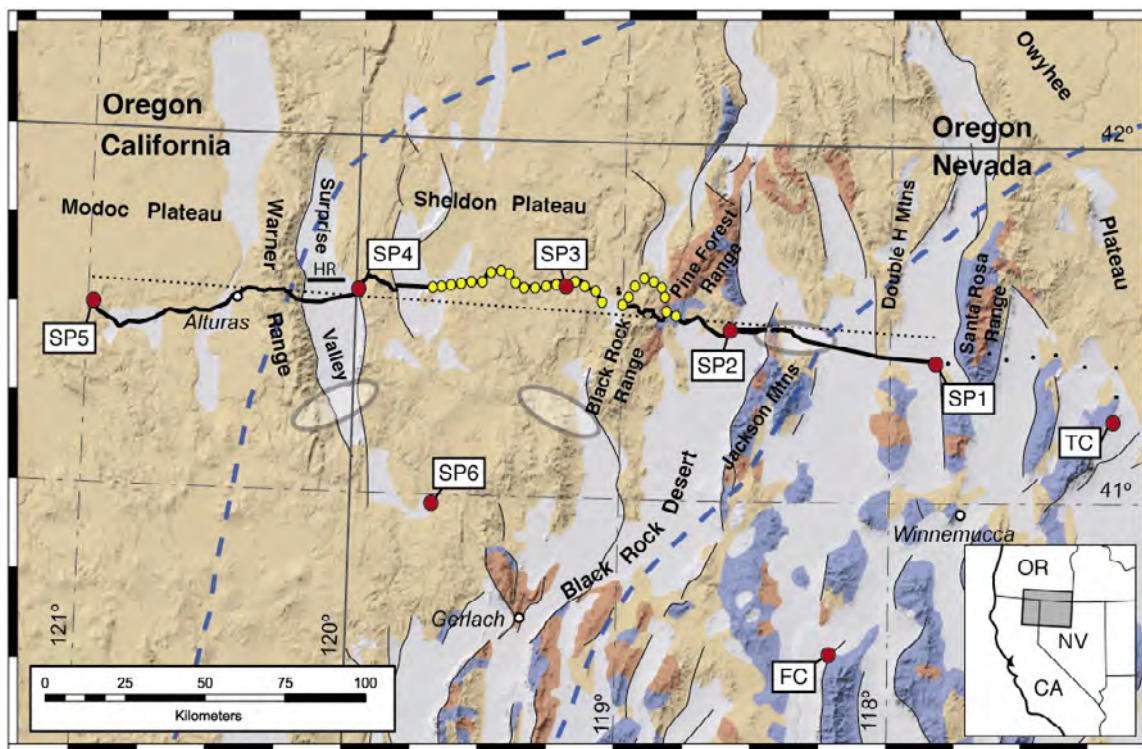


Figure 2. Experiment layout and geology superimposed on a shaded relief map. Gray regions: Quaternary deposits. Tan regions: Tertiary volcanic and sedimentary units. Red regions: Mesozoic granites. Blue regions: Paleozoic and Mesozoic metamorphic units. Thin black lines: significant normal faults. Red circles: shotpoints (SPs 1 and 5, 1800 kg; SPs 2, 3, 4, and 6, 1100 kg) and mine blasts (Twin Creeks (TC) and Florida Canyon (FC) = 68 tonnes and 16 tonnes, respectively). Black circles: geophone locations (appears as a solid line between SPs 1 and 5 due to dense instrument spacing). Yellow circles: passive deployment. Gray ellipses: approximate P_mP bounce points shown in Figure 5. Black dotted line: 2-D gravity profile. HR: Surprise Valley high-resolution reflection profile. Blue dashed lines correspond to basement suggested by *Barton et al.* [1988] to have >50% Cretaceous granitic material. Geology simplified from *Jennings et al.* [1977], *Stewart and Carlson* [1978], and *Walker and MacLeod* [1991].

phism, *Barton et al.* [1988] placed the eastern boundary of the region underlain by >50% Cretaceous batholithic material ~50 km east of the Black Rock Range (Figure 2). The exposed plutons exhibit narrow contact aureoles, typically with andalusite developed [e.g., *Compton*, 1960], suggesting a relatively shallow emplacement level (5–10 km). Thermochronologic data document cooling of the batholith through the ~70°C isotherm (U-Th/He method, ~2–3 km depth) by ~60 Ma [*Colgan et al.*, 2006b]. Continuity of these Paleozoic and Mesozoic rock units within and between ranges, and lack of exposure of deep-crustal levels, support the hypothesis of only limited extension and tilting (and thus exhumation) during Basin and Range faulting [*Colgan et al.*, 2006b].

2.2. Pre-40 Ma: West of the Black Rock Range

[7] The tectonic development of the region west of the Black Rock and Pine Forest Ranges is more

difficult to assess because there are so few pre-Tertiary rocks exposed. Interpolating from the exposures of Mesozoic units both to the east (northwestern Nevada) and west (Klamath Mountains, northeastern California), multiple contractional, accretionary episodes in the Paleozoic and Mesozoic affected this region [e.g., *Ernst*, 1999; *Wylde*, 2002]. This convergent history appears to have ended by the late Cretaceous, because units of this age document the growth of an extensive marine basin. In northern California, the latest-Cretaceous Hornbrook Formation attains a thickness of ~1.5 km [*Nilsen*, 1993]. In southern Oregon, the Eocene Payne Cliffs Formation contains >2 km of predominantly subaerial sandstones and siltstones [*McKnight*, 1984]. This pattern of late Cretaceous-early Cenozoic sedimentation is echoed in the Warner Range (Figure 2), where >1.5 km of cobble conglomerates, volcanoclastic sandstones, lacustrine sediments, and thin basaltic flows underlie ~34 Ma andesites [*Duffield and*

McKee, 1986; Miller *et al.*, 2005]. Although the volcanic flows at the base of this section are as of yet undated, the thickness and mixed composition of the section suggests an extended period of time was required for its accumulation. U-Pb zircon analyses on granitic cobbles from the base of the section were performed on the Stanford-USGS SHRIMP and provided crystallization ages of ~113 and ~171 Ma [Miller *et al.*, 2005]. The ~171 Ma age is a non-unique value for granites in this portion of the U.S. Cordillera, with middle Jurassic plutons present to the east in northwestern Nevada [e.g., Wyld, 1996], to the west in northeastern California [e.g., Irwin, 2003], and to the south in the northern Sierra Nevada [e.g., Girty *et al.*, 1995]. The Cretaceous granitic rocks (~113 Ma) are more diagnostic: they are absent from the Klamath Mountains [Irwin, 2003], but are common in both northwestern Nevada and the northern Sierra Nevada [e.g., Irwin and Wooden, 2001; Colgan *et al.*, 2006b], suggesting the granitic cobbles were sourced from either the south or east. Thus northeastern California (and presumably southern Oregon and northwesternmost Nevada) was a depocenter during the early Cenozoic and accumulated material derived from the east and/or south as the Sierra Nevada batholith became unroofed.

2.3. Eocene-Miocene Volcanism

[8] Multiple volcanic episodes spanned the latest Eocene to middle Miocene across the northwestern margin of the Basin and Range. East of the Sheldon Plateau, sparse 38–35 Ma basalts and basaltic andesites represent the earliest Cenozoic volcanic products [Lerch *et al.*, 2005a; Colgan *et al.*, 2006a]. These units, deposited unconformably on the Paleozoic and Mesozoic granitic, sedimentary, and volcanic rocks described above, have relatively minor amounts of basal topography [e.g., Lerch *et al.*, 2005a], documenting a subaerial and low-relief depositional environment in the latest Eocene. The ensuing volcanic stratigraphy is fairly straightforward: significant bimodal volcanism occurred in two discrete, conformable episodes (26–21 Ma and 16–14 Ma [e.g., Noble *et al.*, 1970; Lerch *et al.*, 2005a; Colgan *et al.*, 2006a]), the latter being largely associated with the McDermitt caldera system and the inception of Columbia River Flood Basalt volcanism [e.g., Zoback and Thompson, 1978; Pierce and Morgan, 1992]. In total, the Cenozoic volcanic section east of the Sheldon Plateau is 1–2 km thick, and is primarily composed of basaltic and rhyolitic prod-

ucts from multiple volcanic episodes that occurred across this region.

[9] Information about the thickness, timing, and composition of the Cenozoic volcanic stratigraphy is limited west of and on the Sheldon Plateau. The most recent volcanic products (usually middle Miocene and younger) are often the only units exposed due to the general absence of large-offset normal faults. In the Warner Range, however, late Eocene (~34 Ma) andesitic flows overlie a very thick early Tertiary sedimentary sequence [Duffield and McKee, 1986]. These Eocene-Oligocene andesites were followed by Oligocene-Miocene basalts and rhyolites [Duffield and McKee, 1986]. Together with interbedded sedimentary units, more than 3 km of material accumulated since ~34 Ma in what later became the Warner Range [Fosdick *et al.*, 2005].

2.4. Neogene Extension in the Northern Basin and Range

[10] Extensional faulting began in the northern Basin and Range in the Eocene, and has continued episodically up to the present day [e.g., Gans *et al.*, 1989; Seedorff, 1991; Christiansen *et al.*, 1992; Wernicke, 1992]. The modern topography of much of the northern Basin and Range formed during a period of large magnitude extension which peaked at about 20–15 Ma [e.g., Miller *et al.*, 1999; Stockli, 1999; Surpless *et al.*, 2002], and coincided with the eruption of the Columbia River flood basalts in Washington and Oregon, and the onset of bimodal basalt-rhyolite volcanism across much of the northern Basin and Range [e.g., McKee, 1971; Stewart and Carlson, 1978; Seedorff, 1991; Christiansen *et al.*, 1992] associated with the Yellowstone hot spot, which is thought to have reached the base of the lithosphere at about 16 Ma beneath McDermitt, Nevada [e.g., Zoback and Thompson, 1978; Pierce and Morgan, 1992; Smith *et al.*, 1993]. Some researchers have suggested that the thermal effects of this plume were responsible for widespread extension across the Basin and Range [e.g., Pierce and Morgan, 1992; Parsons *et al.*, 1994].

[11] Extension began significantly later across the northwesternmost margin of the Basin and Range. Apatite fission-track (AFT) and (U-Th)/He data collected from across northwestern Nevada indicate that extension along the modern range-bounding normal faults began around 12–10 Ma [Colgan *et al.*, 2004, 2006b], later than the 16 Ma inception of volcanism attributed to the Yellowstone plume.

Geologic relationships suggest the 10 Ma - present extension represents the only significant faulting and tilting to affect the region in the Cenozoic [Colgan *et al.*, 2006b]. Thus it appears that Yellowstone hot-spot-related magmatism was accompanied by little or no coeval extensional faulting in the northwestern Basin and Range province. This region must have behaved semi-independently from the central part of the Basin and Range province (~200 km SE), where significant extension by Basin and Range faulting occurred at 17–15 Ma [Stockli, 1999].

2.5. Geophysical Setting

[12] Today, the Basin and Range province is characterized by high average heat flow (~90 mW/m²) and elevated geothermal gradients (~30–40°C/km), although there is considerable local variation within the province (Figure 1) [e.g., Morgan and Gosnold, 1989; Blackwell *et al.*, 1991]. The elevated geothermal gradients implied by high regional heat flow are consistent with typical earthquake focal depths of 10–15 km, and presumably indicate the approximate thickness of the seismogenic crust and depth to the brittle-ductile transition zone.

[13] As seen from regional gravity data, a pronounced isostatic gravity low (~25 mGal) characterizes the northwestern margin of the Basin and Range, with its eastern edge corresponding to the eastern margin of the Sheldon Plateau (Figure 3). Possible tectonic explanations for the gravity low include: a crustal-scale structural boundary [Wylid and Wright, 2001], the granitic Cretaceous arc [Barton *et al.*, 1988], Oligocene-Miocene rhyolitic centers [Noble *et al.*, 1970; Plouff, 1985, 1997; Blakely and Jachens, 1991], or an early Tertiary sedimentary basin. The origin of this ~30 mGal anomaly in northwestern Nevada and northeastern California is discussed in greater detail below.

[14] Figure 1 shows the location of previous seismic reflection and refraction profiles across the northern Basin and Range that provide data on crustal thickness and velocity structure across the region. The best data come from the COCORP (Consortium for Continental Reflection Profiling) 40°N deep seismic reflection profiles [e.g., Allmendinger *et al.*, 1987; Klemperer *et al.*, 1986] and the 1986 PASSCAL Basin and Range Lithospheric Seismic Experiment [e.g., Jarchow *et al.*, 1993; Catchings and Mooney, 1991]. The COCORP and PASSCAL data are augmented by passive imaging of the eastern Basin and Range [Gilbert and Sheehan, 2004], refraction/

reflection imaging along the Ruby Mountains [Stoerzel and Smithson, 1998], and a coarse refraction survey across western Nevada and eastern California [Louie *et al.*, 2004]. The crust varies in thickness from 34 km in central Nevada to ~30 km at 40°N in northwestern Nevada and western Utah (Figure 1), and has been interpreted to be underlain by a high-velocity ($V_p \sim 7.4$ km/s) “rift pillow” [e.g., Catchings and Mooney, 1991] across much of northwestern Nevada. The reflection profiles show a relatively sharp Moho across the entire Basin and Range, with subhorizontal reflectivity in the middle and lower crust [e.g., Holbrook *et al.*, 1991; Klemperer *et al.*, 1986]. These features are now recognized as characteristic of extended terranes worldwide, and have led numerous workers to a now widely accepted model of continental extension in which spatially varying amounts of upper-crustal extension are accommodated by more uniform ductile flow and thinning in the middle and lower crust [e.g., Gans, 1988; Block and Royden, 1990; McKenzie *et al.*, 2000].

3. Data Acquisition and Processing

3.1. Seismic Data

[15] In September 2004, we completed a ~300 km active-source seismic survey as part of the Earthscope program and with funding from the Petroleum Research Foundation. Five in-line shots, and one off-line fan shot (shot sizes 1100 to 1800 kg) were recorded by ~1100 vertical seismometers (Figure 2). These data were augmented by two additional blasts at the Twin Creeks (in-line) and Florida Canyon (off-line) mines (TC and FC, Figure 2). These much larger shots (75 tons and 15 tons, respectively) were ripple-fired, producing long source signatures that make their recordings useful only for first-arriving energy. Approximately 35 km of vibrator-source data using the Network for Earthquake Engineering Simulation (NEES) Tri-Axial “T-Rex” vibrator (267 kN peak force, 60 s sweeps, 5–40 Hz) provide useful first-arrivals at near offsets (~25 km) but were too widely separated to allow creation of a stacked reflection profile. While the bulk of the recording was done by self-contained, single channel Reftek RT125s (Texans), we also used Reftek RT130 multi-channel digitizers with short-period (4.5 Hz) three-component sensors to provide an additional 114 channels. We relied largely on PASSCAL equipment provided within the framework of Earthscope, resulting in station spacing that was nominally 300 m, but

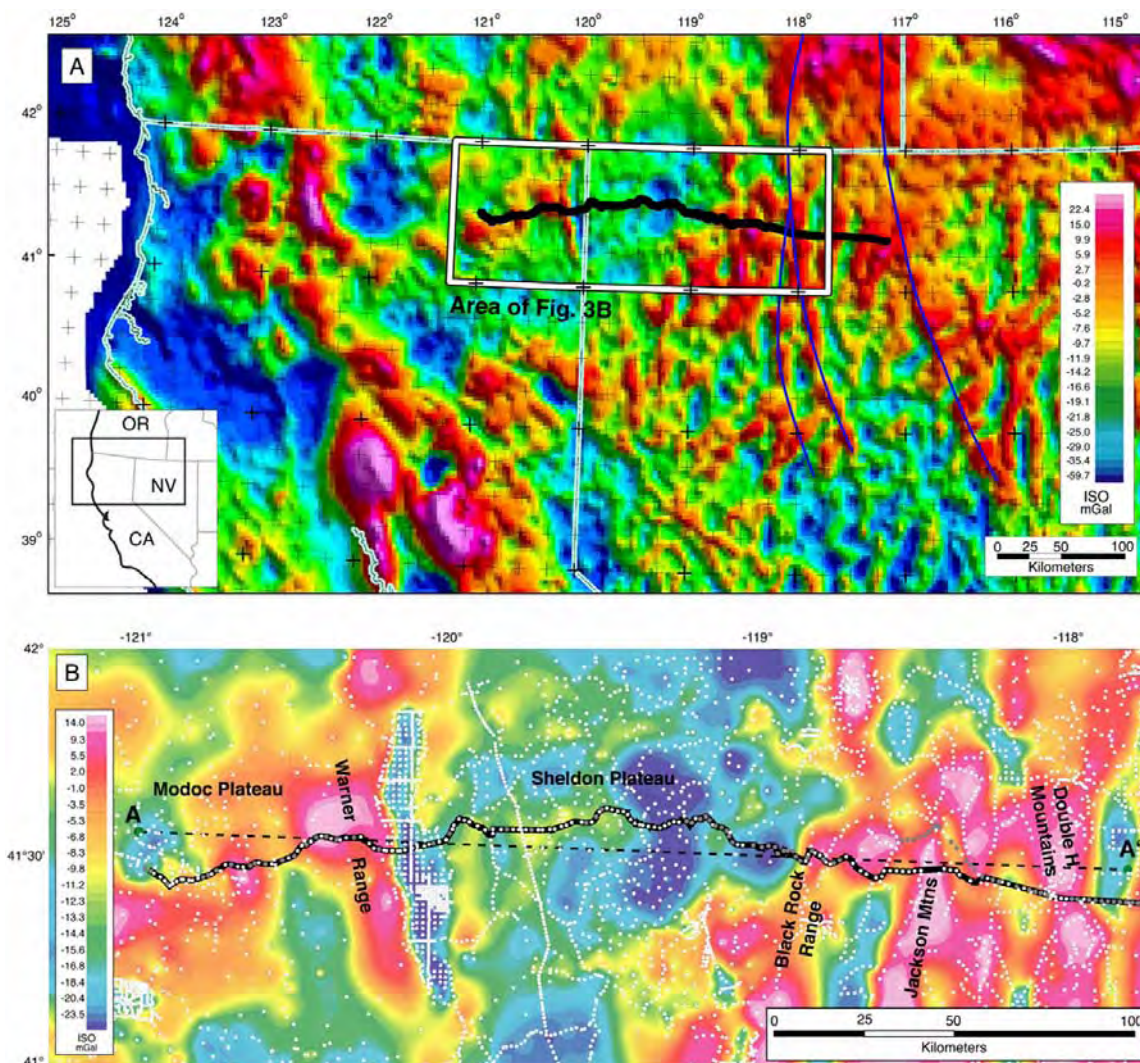


Figure 3. Regional isostatic gravity: complete Bouguer gravity corrected for the effects of Moho topography assuming an Airy-Heiskanen isostatic compensation model with a crustal density of 2.67 g/cm^3 , and a density contrast across the Moho of 0.4 g/cm^3 . (a) Isostatic gravity for the northwestern Basin and Range and neighboring regions. Heavy black line: refraction profile. Thin blue lines: middle Miocene basaltic dike swarms (Northern Nevada Rifts). (b) Isostatic gravity for region immediately surrounding our seismic profile. White circles: existing gravity stations. Gray circles: 84 gravity stations collected here. Dashed black line A-A': gravity model profile of Figure 8. Heavy black line: path of receivers from the refraction survey.

included a denser recording interval (100 m) over the central $\sim 35 \text{ km}$ of the line (western edge of the Black Rock Range to the Jackson Mountains, Figure 2). A $\sim 10 \text{ km}$ gap in the recording line occurs at the Summit Lake Indian Reservation just west of the Black Rock Range (Figure 2). Only sparse recorders ($\sim 5 \text{ km}$ spacing) were deployed between Shotpoint 1 and the Twin Creeks Mine, because the latter represented a shot of opportunity that had not been guaranteed to take place during our recording windows. All data were pre-processed by PASSCAL and are archived at the IRIS Data Management Center (DMC). Our project

also included a 7-month deployment of short-period passive instruments for teleseismic recording in the central portion of our profile [Gashawbeza *et al.*, 2005], and a high-resolution shallow penetration Vibroseis reflection profile across Surprise Valley [Lerch *et al.*, 2005b] (Figure 2). In this paper, we utilize only the vertical component data as S-wave energy from our controlled sources was disappointingly absent. The passive-source and reflection data are left as the subjects of separate studies [Gashawbeza *et al.*, 2005; Lerch *et al.*, 2005b].

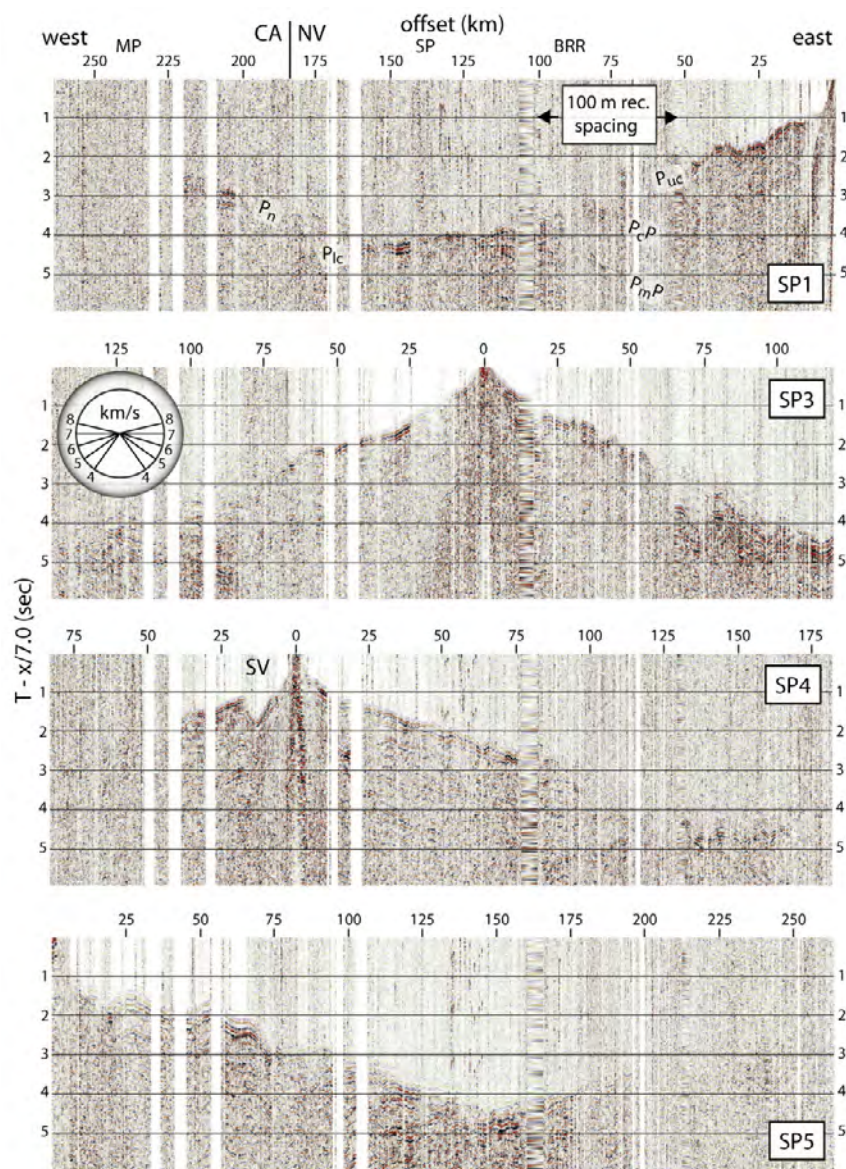


Figure 4. Shot gathers from Shotpoints 1, 3, 4, and 5. All gathers reduced at 7.0 km/s; velocity wheel in Shotpoint 3 gather shows slopes of arrivals of velocities from 4 to 8 km/s. Data processing described in text. MP, Modoc Plateau; SP, Sheldon Plateau; BRR, Black Rock Range. SV in SP4: Surprise Valley pull-down described in text.

[16] The gathers from the in-line shots show clear first arrivals to offsets from 150 to 200 km (Figure 4, note that Shotpoint 2 failed and produced no useful data). Low surface velocities are evident on all gathers, with an extreme velocity pull-down present in Surprise Valley (see Shotpoint 4, Figure 4). The upper-crustal refracted phase ($P_{uc} \sim 6$ km/s) is observed on all gathers, and is the first arrival to greater offsets at the western end of the survey (~ 150 km for Shotpoint 5) than the eastern end (~ 100 km for Shotpoint 1). A clear lower-crustal refracted phase (P_{lc}) was recorded from Shotpoints

1, 3, and 4, but is obscured at the P_n crossover distance from Shotpoint 5 (Figure 4). Refracted Moho arrivals (P_n) are visible on Shotpoints 1 and 5, as well as from the Twin Creeks mine blast (not shown). There are very few intra-crustal reflections visible in the data, of which the most convincing is a mid-crustal reflection (P_cP) observed under the eastern end of the survey in the region of 100 m receiver spacing (Figures 4 and 5, Shotpoint 1).

[17] Data processing consisted of established techniques: picking observed phases, forward modeling for first-order fit, and inversions for more complete

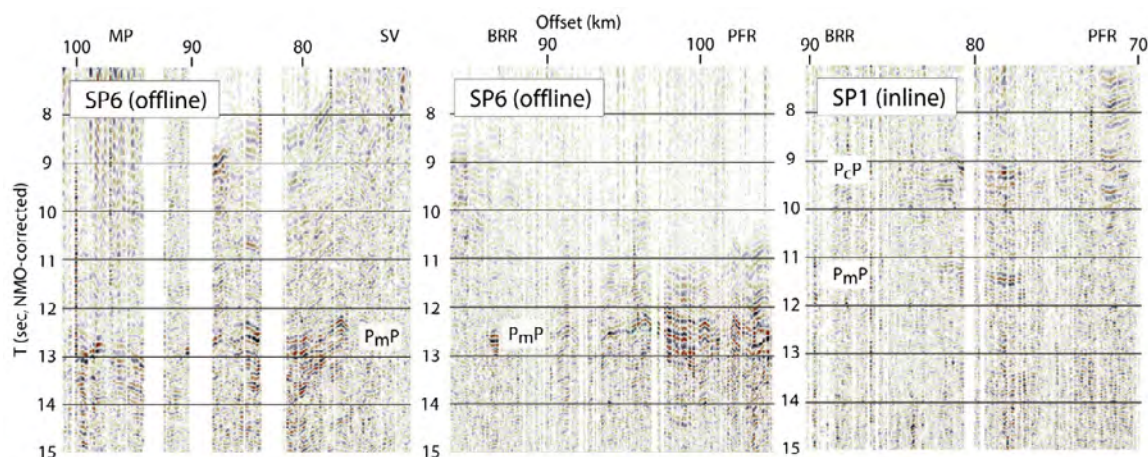


Figure 5. Shot gathers with NMO applied using a 1-D correction velocity profile derived from average values of the velocity model. Left panel shows P_mP arrival at Surprise Valley (SV) and the Modoc Plateau (MP) from Shotpoint 6 (offline fan shot). Center panel shows P_mP arrival at the Black Rock Range (BRR) and southern end of the Pine Forest Range (PFR) from Shotpoint 6 (offline fan shot). Right panel shows P_mP and P_cP arrivals at the Black Rock Range (BRR) and the southern end of the Pine Forest Range (PFR) from Shotpoint 1 (inline). Bounce point locations shown in Figure 2. (Note: horizontal scale varies between figures.)

traveltime agreement. Traveltime-modeling was followed by amplitude and gravity modeling to confirm the major features of the model. A band-pass filter (corner frequencies of 2, 4, 10, and 16 Hz) and a minimum phase predictive deconvolution (500 ms operator length, 50 ms prediction distance, 0.1% pre-whitening) were applied to all shot gathers. Pick uncertainties varied from 75–150 ms, depending on arrival clarity. The velocity model is constrained by 2192 picks (Table 1) from the in-line shot gathers (Figure 4), with an additional 515 picks from the vibrator-source (T-Rex) gathers that illuminate the surface velocities in the vicinity of the Black Rock and Pine Forest Ranges (Figure 2). In our forward modeling, we used Modeling (a GUI by Gou Fujie based on Colin Zelt’s RayInvr) to establish a starting model and obtain a reasonable fit to the data. Inversions were then computed with RayInvr [Zelt and Smith, 1992] by using a layer-stripping approach [Zelt *et al.*, 1993] to arrive at a final model that adequately fits the observed arrivals (Figures 6 and 7). Six raygroups (P_{sur} , P_{uc} , P_cP , P_{lc} , P_mP , and P_n) were used in the velocity modeling and included both primary and secondary arrivals.

3.2. Potential Field Data

[18] We collected 84 new gravity stations (average spacing ~ 3 km) along the seismic line and compiled these with the existing regional coverage [Snyder *et al.*, 1981; Ponce, 1997] to produce a grid from which we interpolated a profile for

potential-field modeling. New gravity data were reduced using standard gravity methods [Blakely, 1995] that include: earth-tide, instrument drift, latitude, free-air, simple Bouguer, curvature, terrain, and isostatic corrections to yield the complete Bouguer (CBA) and isostatic anomalies. A straight-line two-dimensional profile of the CBA that coincides with the seismic profile and is roughly perpendicular to the strike of geologic structure was extracted from the gravity grid (dotted line, Figure 2) and forward modeled [Talwani *et al.*, 1959; Blakely and Connard, 1989] using GMSYS software. Velocity-to-density mapping consisted of converting P-wave velocities to densities by using the [Brocher, 2005] modification of the Nafe-Drake relationship [Ludwig *et al.*, 1970] that seeks a best average velocity-to-density conversion applicable to a broad range of common rock types.

[19] At the regional scale, the profile is characterized by three distinct gravity domains (Figure 8):

Table 1. Velocity Modeling Results for Observed Phases

Phase	Picks (Used/Made)	RMS Residual, sec	χ^2
$P_{surface}$	39/62	0.103	1.953
$P_{upper\ crust}$	1515/1522	0.114	1.242
P_cP	14/14	0.069	0.225
$P_{lower\ crust}$	202/215	0.094	0.862
P_mP	115/119	0.139	0.872
P_n	258/260	0.155	0.980
Total	2142/2192	0.120	1.181

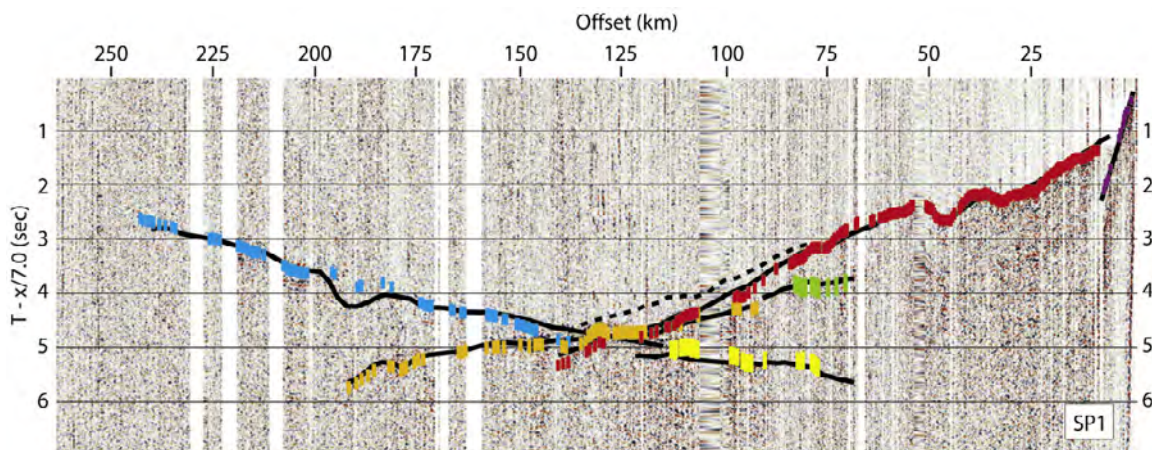


Figure 6. Reduced shot gather from Shotpoint 1 (LMO = 7.0 km/s). Phase picks (colored vertical bars show assigned uncertainties) and modeled arrivals (black lines) are superimposed on data. Dashed black line from offsets of 75–130 km represents modeled P_{uc} arrivals produced by increasing upper-crustal velocities near the Black Rock Range by 0.2 km/s (see text for discussion). Phase color scheme: magenta ($P_{surface}$), red ($P_{upper\ crust}$), green (P_cP), orange ($P_{lower\ crust}$), yellow (P_mP), and blue (P_n).

two relatively equal Bouguer highs (~ -160 mGal) at either end of the profile and a broad central negative anomaly (~ -190 mGal) that is separated from the western and eastern highs by short-wavelength gradients. Included in Figure 8 is the Bouguer anomaly (~ 70 mGal, see dotted line) arising from the velocity-derived Moho topography assuming a

$\Delta\rho = 0.4$ g/cm³ increase across the Moho. This eastward-increasing variation is counteracted by the laterally varying velocity and density structure of the crust which has higher values at the western end of the survey than to the east. Densities calculated from our seismic model (discretized at 0.2 km/s velocity intervals) provide a reasonable fit between observed

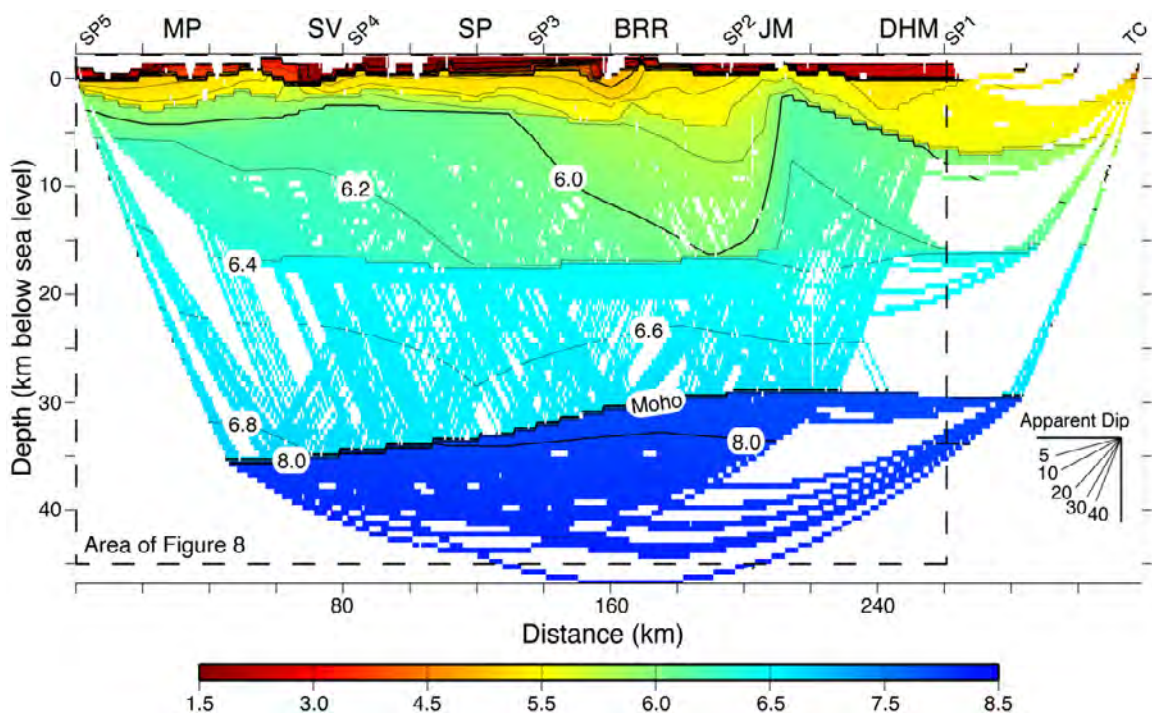


Figure 7. Final velocity model. Velocities displayed in km/s, contoured every 0.2 km/s (heavy contours every 1.0 km/s). Geographical features labeled (MP, Modoc Plateau; SV, Surprise Valley; SP, Sheldon Plateau; BRR, Black Rock Range; JM, Jackson Mountains; DHM, Double H Mountains). Shotpoints (SP) 1–5 and Twin Creeks (TC) mine blast are labeled. V.E. 3:1.

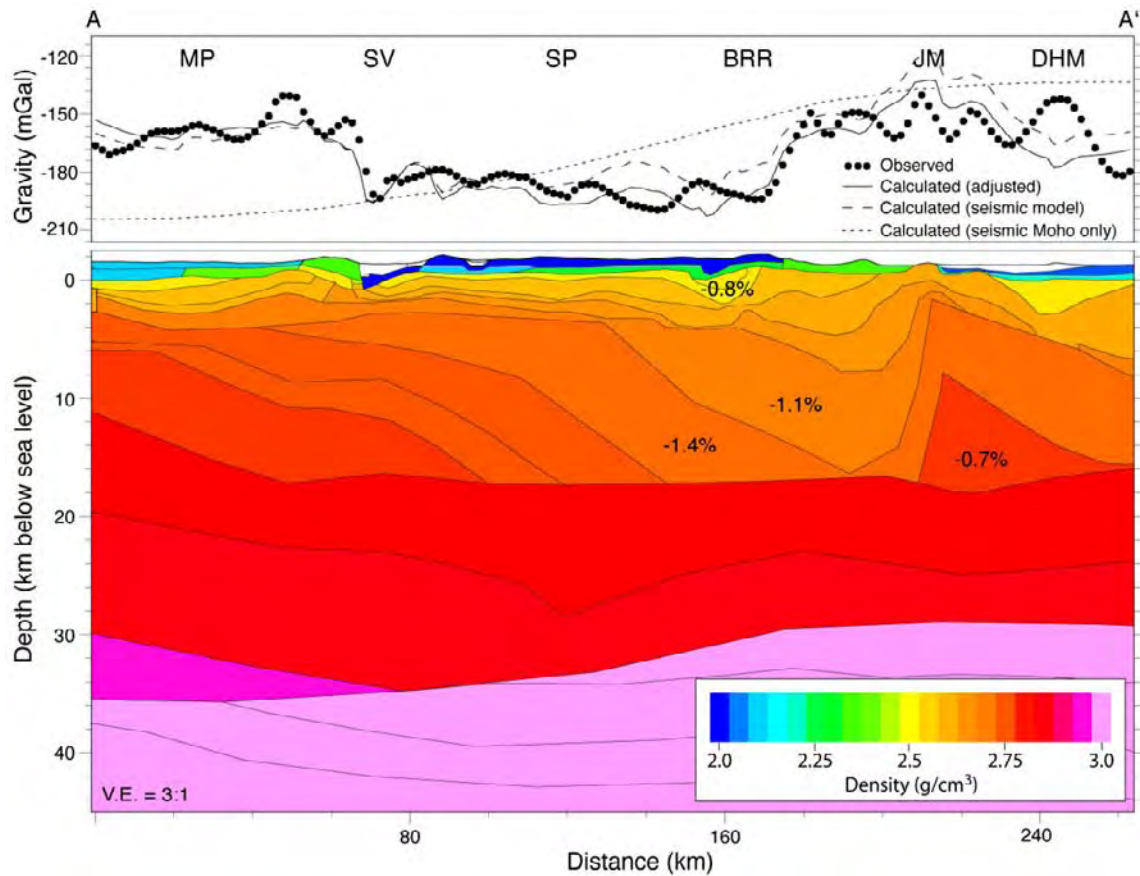


Figure 8. Comparison of observed Bouguer gravity (black circles) with that predicted by various density models. Short dashed line: modeled Bouguer anomaly with no lateral density heterogeneities other than Moho topography ($\Delta\rho = 0.4 \text{ g/cm}^3$) taken directly from the seismic model (Figure 7). Long dashed line: predicted Bouguer anomaly from directly mapping V_p to density using the modified Nafe-Drake approximation of Brocher [2005]. Solid line: predicted Bouguer anomaly from modified density structure, with density modifications labeled on figure in percent change from the Brocher [2005] approximation (e.g., -1.1% between BRR and JM corresponds to reducing density from 2.70 to 2.67 g/cm^3). Geographical features labeled are as follows: MP, Modoc Plateau; SV, Surprise Valley; SP, Sheldon Plateau; BRR, Black Rock Range; JM, Jackson Mountains; DHM, Double H Mountains.

and predicted data (long dashed line, Figure 8). This gravity signature is broadly matched by our velocity-density conversion, showing all three major trends, and relatively sharp gradients on either side of the central negative anomaly.

[20] A modified density model provides an improved fit to the observed values, and was produced by reducing density values (never by more than 1.5% , or 0.04 g/cm^3) while maintaining the geometry of the density structure exactly as constrained by the velocity model (Figure 8). This modified density model more accurately matches both the sharp gradient on the eastern edge of the Sheldon Plateau, and the gravity signal near the Jackson Mountains. In producing this modified density model, we changed a minimum number of values, seeking only a first-order fit to the data. Despite the broad agreement between our modeled

and observed densities, persistent misfit of the short-wavelength signals ($<20 \text{ km}$) between the observed and modeled gravity are seen in both the Warner Range and Double H Mountains (Figure 8). At the eastern end of the gravity profile, a $\sim 30 \text{ mGal}$ positive anomaly that is not accounted for by the model occurs over the Double H Mountains. Inspection of the 2-D gravity profile location (Figure 2) explains much of this incompatibility: the gravity profile crosses the southern end of the Double H Mountains, whereas the seismic data is confined to the basin at the southern end of the range. Focused mafic dikes of the westernmost arm of the northern Nevada rift trend SSE through the Double H Mountains (Figure 3), accounting for an additional $\sim 5\text{--}8 \text{ mGal}$ [Zoback *et al.*, 1994] of the positive anomaly in this portion of the model.

To the west in the Warner Range, a ~ 12 mGal positive disparity is centered on the western edge of the range, and marks the southern end of a spatially limited and poorly defined (poor data coverage) gravity high (Figure 3b) associated with Tertiary intrusive rocks [Chapman and Bishop, 1968]. We interpret this disagreement between the observed and modeled data sets to be related to a mismatch in survey locations, as the seismometers on either side of this gravity high were positioned south of the anomaly, meaning that many of the raypaths traveling to these stations failed to sample the source body.

[21] Several additional models (not shown here [Glen *et al.*, 2005]) were developed (independent of the seismic velocity structure and velocity-derived densities) through simultaneous forward modeling of gravity and magnetic data to match the calculated anomalies with observed anomalies while taking into account constraints imposed by surface geology, rock property data, and geophysical data. Density and magnetic properties of bodies were adjusted iteratively to match observed and calculated gravity and magnetic profiles. These models confirm the fundamental results presented here: that the steepest seismic velocity gradients occur at shallow to mid-crustal levels at the margins of the anomalous gravity low.

4. Crustal Structure and Average Velocities and Densities

4.1. Crustal Thickness and Reflectivity

[22] Crustal thickness is constrained both by P_mP and P_n arrivals in the seismic data, and varies from ~ 38 km under the western, unextended end of the survey, to ~ 32 km to the east (Figure 7). These Moho depths agree with earlier studies from northwestern Nevada (COCORP 40°N and 1986 PASSCAL) and northeastern California (1981 USGS), confirming the change in crustal thickness across the western margin of the Basin and Range province. P_mP and P_cP arrivals are most coherent under the eastern portion of the line (see Figure 5, right panel) where we deployed instruments at 100 m spacing, yet present a contrasting image of crustal reflectivity when compared to previous surveys from more highly extended portions of the Basin and Range. In particular, distributed lower-crustal reflectivity is missing from the crustal column under northwesternmost Nevada. Because our Shotpoint 2 (Figure 2) failed, we recorded no near-offset explosion data with our most densely

spaced receivers, obviating an absolute comparison of reflectivity between our survey and the remarkable middle- and lower-crustal reflectivity observed in the 1986 PASSCAL survey [Catchings and Mooney, 1991]. A comparison of relative amplitude against time for our data (SP1) and for the 1986 PASSCAL experiment (their SP4) [Catchings and Mooney, 1991, Figure 11a] is shown in Figure 9. At near-offsets (10–15 km), the relative amplitude (a proxy for signal-to-noise ratio) in both our data and in the 1986 PASSCAL survey show continuing amplitude decay to ~ 10 s, which is the standard test for signal propagation to depths equivalent to those traveltimes. Thus absence of evidence for reflectivity is, in this case, evidence of absence.

4.2. Near-Surface Velocities and Densities

[23] Velocities and densities within ~ 2 km of the surface are particularly low ($V_p \leq 3$ km/s, $\rho \leq 2.3$ g/cm³) between the Black Rock Range and Surprise Valley (Figures 7 and 8), corresponding to the topographically high Sheldon Plateau (Figure 2), despite the fact that outcrops are dominated by basalts and welded ash-flow tuffs. Large-offset normal faults are absent on the Sheldon Plateau, leaving only the youngest volcanic rocks visible at the surface. Insight into the subsurface lithologies across this region comes from large tilted fault blocks on its eastern and western margins that expose deeper structural levels. To the east, the Black Rock Range (Figure 2) is a gently dipping horst block that preserves a remarkably complete section of Tertiary volcanic rocks [Lerch *et al.*, 2005a]. In the ~ 1 km volcanic section of the northern Black Rock Range, roughly 60–70% is composed of slope-forming, unwelded volcanic units. On the western margin of the Sheldon Plateau, the Surprise Valley fault exposes nearly 2 km of Tertiary sedimentary and volcanoclastic deposits [Duffield and McKee, 1986; Carmichael *et al.*, 2006]. Hence, although basalts and variably welded ash-flow tuffs dominate the surface of the Sheldon Plateau, the bulk of the underlying Tertiary section is inferred to consist of sedimentary and unwelded silicic volcanic deposits (Figure 7) and is likely responsible for much of the gravity low across this region (km 85 to 155 in Figure 8).

4.3. Upper-Crustal Velocities and Densities and the Sierra Nevada Batholith

[24] Upper-crustal velocities are laterally heterogeneous across the study area, with the most pronounced anomaly present in the central portion of

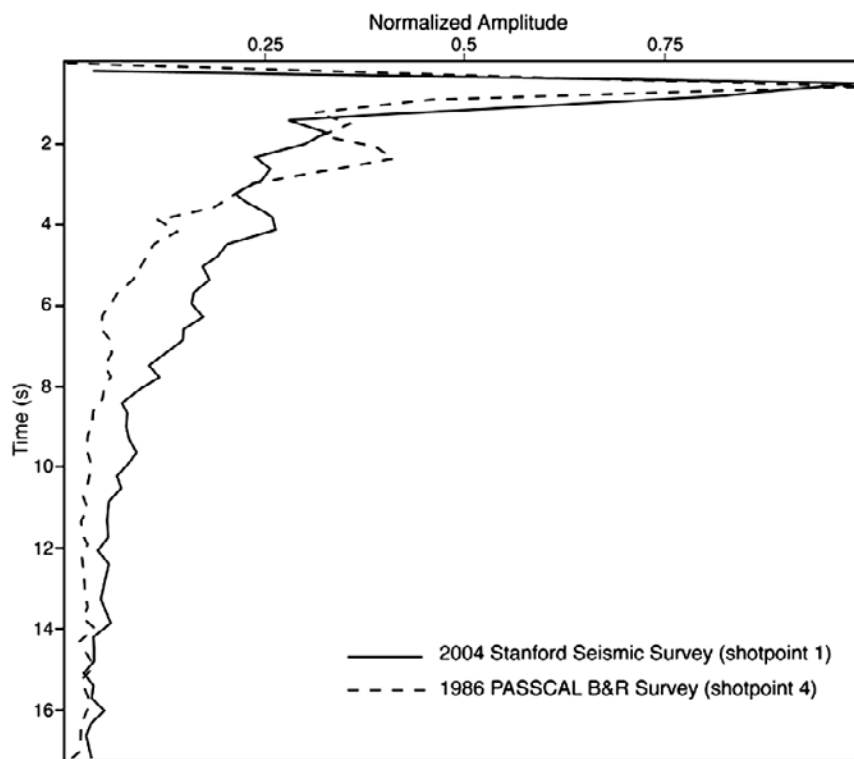


Figure 9. Amplitude comparison between our survey and the 1986 PASSCAL Basin and Range experiment. Each amplitude-decay curve was produced by taking the Hilbert transform of the original data, summing over adjacent traces at source receiver offsets from 10–15 km, and then plotting the amplitude as a function of time.

our profile near the Black Rock Range and Jackson Mountains (Figure 7). Iso-velocity contours in this part of the model dip steeply inward from the west and east, defining a 15 km-thick region of low velocities ($V_p \sim 5.8\text{--}6.1$ km/s) that occurs beneath exposed Jurassic and Cretaceous granitic rocks that have been interpreted to mark the trace of the Sierran batholith as it passes through northwestern Nevada (Figure 2) [Barton *et al.*, 1988]. It is worth noting that eastern edge of our low-velocity depression agrees reasonably well with the estimates from Barton *et al.* [1988] (Figure 2). We attribute the discrepancy on the western edge to the absence of surface exposures of pre-Tertiary rocks available to Barton *et al.* [1988] when they constructed their boundaries (Figure 2). Our low-velocity depression is robustly imaged: an increase in V_p of 0.2 km/s, still not enough to make this region have globally average upper-crustal velocities, would predict far earlier traveltimes than the error bounds of our interpretations (Figure 6). This low-velocity upper crust spans ~ 100 km (Figure 7), equivalent to the surface outcrop of the Sierra Nevada batholith in central California, and shows even lower seismic velocities than the anomalously low-velocity crust in the southern Sierra Nevada (Figure 10) [Fliedner

et al., 2000]. This region near the Black Rock and Pine Forest Ranges also presents the greatest discrepancy in our gravity modeling (Figure 8), and a better fit to the gravity data was obtained by using densities slightly lower than predicted by the [Brocher, 2005] approximation. Densities predicted from V_p using the Nafe-Drake or Brocher conversions which average all rock types are expected to be systematically high (~ 0.06 g/cm³ or $\sim 2\%$) for granitic-granodioritic lithologies [Christensen and Mooney, 1995], strengthening the case for granitic material in this region. Non-granitic velocities (≥ 6.4 km/s) below the mid-crust in our study area indicate that either the lower crust has been substantially altered by Cenozoic magmatism, or that Cretaceous arc magmatism in this portion of the Cordillera was lower in magnitude than in the southern Sierra Nevada. While the absence of reliable seismic velocity information anywhere between our survey and the southern Sierra Nevada makes it difficult to draw an absolute correlation between these two data points ~ 500 km apart, we conclude on the basis of the available geologic and geophysical information that we have better described the location and extent of the Cretaceous arc in a region

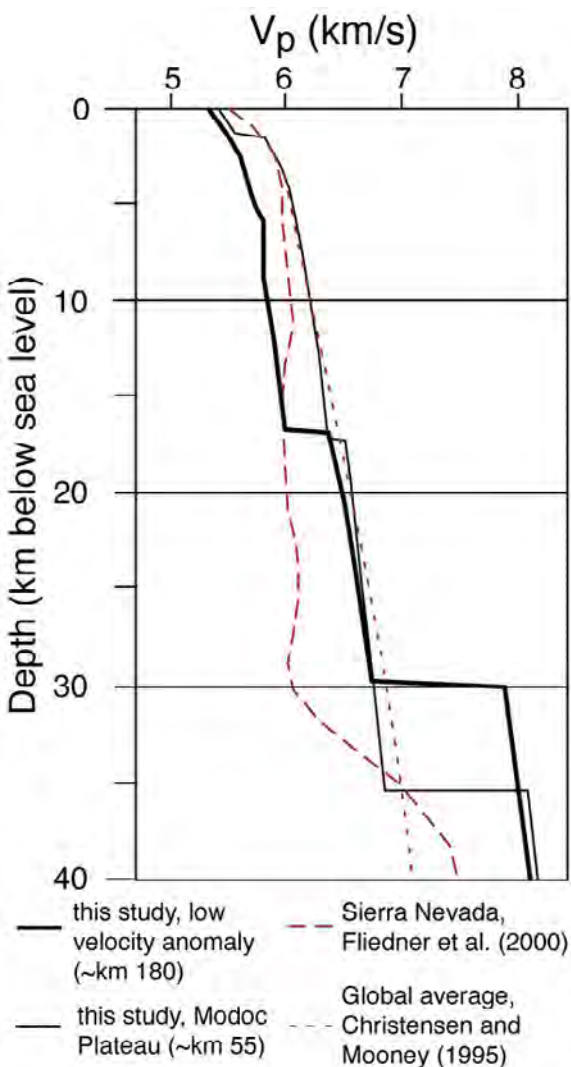


Figure 10. One-dimensional velocity profiles. Heavy solid line: velocity profile from the region around Black Rock and Pine Forest Ranges. Thin solid line: velocity profile from the Modoc Plateau. Red dashed line: velocity profile from central portion of the southern Sierra Nevada [Flidner *et al.*, 2000]. Red dotted line: global average [Christensen and Mooney, 1995].

where its location had formerly been incompletely understood.

4.4. Lower-Crustal Velocities

[25] Lower-crustal velocities increase from east to west across the northwestern Basin and Range transition zone, from 6.4 to 6.75 km/s under the eastern end of the survey, to 6.5 to 6.85 km/s under the Modoc Plateau (Figure 7). This increase in lower-crustal velocities (and presumably densities) counteracts the reduced gravity contribution from the thickened crust to the west, helping maintain

the relatively uniform Bouguer anomaly measured at the eastern and western ends of the survey (Figure 8). Of note here is the absence in our interpretation of a discrete lower-crustal “7.x” km/s layer, commonly attributed to the presence of magmatic underplating [e.g., Catchings, 1992] and perhaps related to a zone of enhanced near-vertical reflectivity at the base of the crust [Klemperer *et al.*, 1986]. Independent modeling of the 1986 PASSCAL survey (~130 km south of our survey, Figure 1) produced two separate interpretations of the velocity structure of western Nevada, one with and one without a lower-crustal 7.x layer (Catchings and Mooney [1991] and Holbrook [1990], respectively). Catchings and Mooney [1991] interpreted westward-thickening of the 7.x layer along the NW-SE PASSCAL transect, from ~1 km in central Nevada, to ~7 km in northwestern Nevada. In his interpretation paper on the COCORP and PASSCAL surveys, Catchings [1992] suggested the 7.x velocities in western Nevada correspond to the addition of mantle-derived melts to the base of the crust during Basin and Range rifting. Because we have not worked directly with the 1986 PASSCAL data set, we do not comment on the validity of the 7.x layer in western Nevada, but we do note that the Catchings [1992] interpretation of large magnitude mafic underplating in western Nevada in response to continental rifting is surprising due to the relatively minor amount of upper-crustal extension in this region ($\leq 30\%$ [Colgan *et al.*, 2006b]) when compared to the more highly extended central part of Nevada ($>50\%$ extension [Smith *et al.*, 1991]). Although our traveltimes modeling requires no high-velocity underplate in our study area, inevitably there is some uncertainty because of the finite-frequency of our seismic waves which have wavelengths of up to 1.5 km in the lower crust. Amplitude modeling of P_mP reflections suggests the Moho may be gradational over 1 to 2 km, possibly caused by extremely mafic cumulates, or by inter-layered mafic and ultramafic materials at the base of the crust (Figure 11). Upon comparing synthetic seismograms (Figure 11) with the observed data (Figure 4), it appears that a somewhat gradational Moho may more accurately reproduce the observed P_mP phase on Shotpoint 1, which we can only trace to offsets of <200 km (arrivals “D”, Figure 11). Adding a strongly gradational Moho, however, introduces a reflection (arrival “C”, Figure 11) that is clearly intermediate between P_cP and P_mP , and is not seen in the data set (Figures 4 and 5). We conclude that the observed absence of both a 7.x refracted phase and a reflection from the top of this

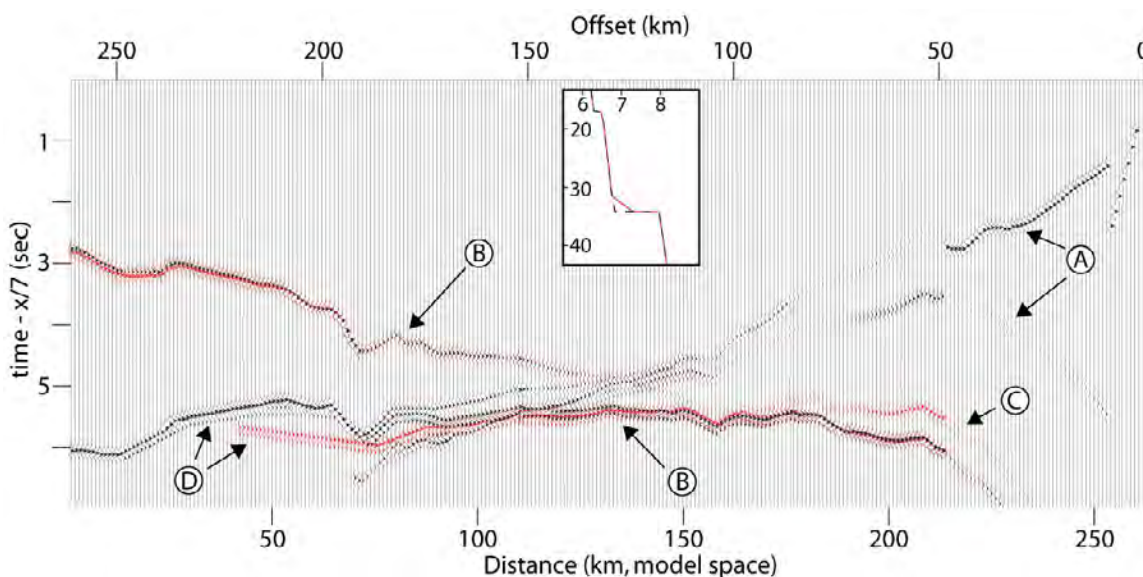


Figure 11. Synthetic seismogram for Shotpoint 1 (using code of *Zelt and Smith* [1992]). Black: seismogram produced with best-fit velocity model (Figure 7). Red: seismogram produced with gradational Moho to simulate distributed mafic addition to the base of the crust (abrupt velocity jump in Figure 7 is artificially spread out over 3 km). Inset figure shows 1-D velocity profiles for best-fit model (black dashed line) and gradational Moho model (red line). “A” arrivals do not interact with the crust-mantle interface and are identical in the two seismograms. “B” arrivals have similar arrival times and waveforms in both models. “C” arrivals show that a gradational Moho should give additional reflectivity above the main P_mP that is not observed in our data set. “D” arrivals represent a mismatch between the two models, described in the text.

interface, dictates that if a high-velocity mafic underplate exists under our survey area, it is minor in magnitude (<3 km). Thus, although the extensional and magmatic histories surveyed by 1986 PASSCAL and our experiment are comparable, the addition of a mafic underplate may not have been uniform.

4.5. P_n Velocities

[26] Observed P_n velocities increase from east (~7.95 km/s) to west (~8.05 km/s) across our survey, possibly corresponding to elevated lithospheric mantle temperatures under the Basin and Range. A 0.1 km/s increase in velocity is about double that expected due to the ~5 km increase in Moho depth (and corresponding increase in pressure) and may indicate a decrease in temperature of ~100°C. This variation in P_n agrees qualitatively with recent work in our study area that constrains depth to the lithosphere-asthenosphere boundary at ~60 km in northwestern Nevada (X. Li et al., The lithosphere-asthenosphere boundary beneath the western United States, submitted to *Geophysical Journal International*, 2007) and ~70 km in northeastern California. Our P_n velocities are slightly below the global average [e.g., *Christensen and Mooney*, 1995] and fit well with other seismic experiments from across the northern Basin and

Range [*Catchings and Mooney*, 1991], consistent with above-average heat flow and below-average crustal thickness of this province (Figure 1). The homogeneity of Basin and Range Moho velocities suggests that composition and state of the lithospheric mantle is moderately uniform despite local heterogeneities in surface heat flow [e.g., *Blackwell et al.*, 1991] and magmatism [e.g., *Best et al.*, 1989].

5. Tectonic Implications

[27] Together with the geologic history preserved at the surface, our geophysical data have broad implications for the tectonic development of the northwestern Basin and Range and its transition to unextended crust in northeastern California and southeastern Oregon. Working backward in time from the most recent tectonic activity, we reconstruct the major tectonic and magmatic events, and provide an interpretation of the crustal evolution of our study area from the late Cretaceous through the Cenozoic (Figure 12).

5.1. Tectonic Reconstruction at 13 Ma

[28] As described above (Regional Geology and Geophysics), Basin and Range extension in north-

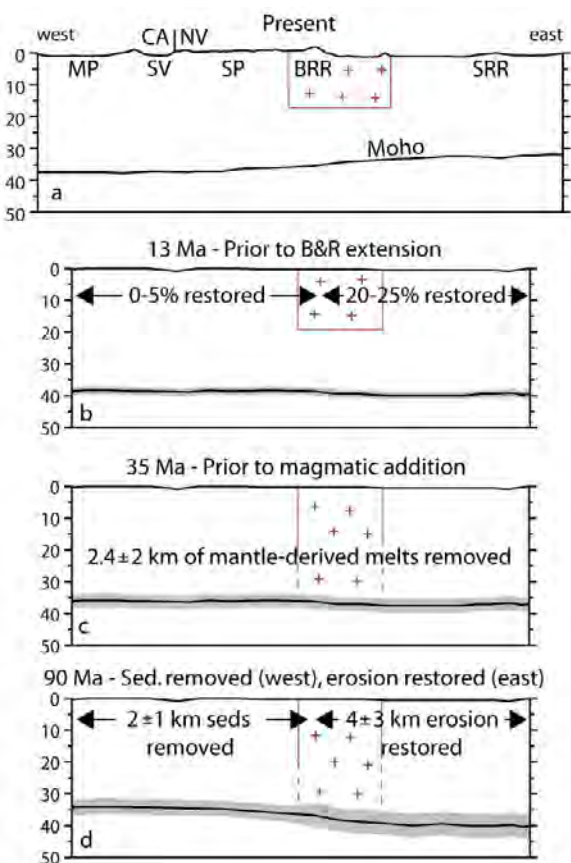


Figure 12. Schematic crustal evolution from late Cretaceous-present. (a) Present-day crustal structure with west-dipping Moho, lower- and mid-crustal magmatic addition, and modern topography (MP, Modoc Plateau; SV, Surprise Valley; SP, Sheldon Plateau; BRR, Black Rock Range; SRR, Santa Rosa Range). Red crosses: region of low V_p inferred to mark location of the Sierra Nevada batholith. (b) Crustal structure before Basin and Range extension; Moho topography is reduced. (c) Removing Cenozoic magmatic addition thins crust. Prior to magmatic addition, region of low V_p inferred to represent the Sierra Nevada batholith that may extend through the entire crust. (d) Restoring erosion (east) and removing sedimentation (west) produces an east-dipping Moho. Reconstruction uncertainty (RMS) is represented by the gray Moho outline. V.E. $\sim 2:1$; topography is shown schematically.

western Nevada and northeastern California began at ~ 12 – 10 Ma, and has accommodated a stretching total of 20–25% east of the Sheldon Plateau, with 0–5% extension west of the Black Rock and Pine Forest Ranges (Figure 2). The magnitude of upper-crustal extension recorded at the surface is roughly consistent with the degree of eastward crustal thinning across this transition zone, and suggests the response to Basin and Range extension has been relatively uniform over the entire

crustal column. This relationship is straightforward when compared to other portions of the northern Basin and Range, where the heterogeneous nature of upper crustal deformation contrasts with the homogeneous strain observed in the lower crust [e.g., Gans, 1988]. This inferred decoupling between upper and lower crustal deformation, considered responsible for the absence of high-amplitude Moho relief [e.g., Klemperer *et al.*, 1986] despite large local variations in upper-crustal extension, is not required in our survey area. By restoring extension across the survey region, the lateral change in crustal thickness is effectively removed and provides an estimated Moho depth of $\sim 38 \pm 1$ km (Figure 12b) prior to the inception of Basin and Range faulting.

5.2. Tectonic Reconstruction at 35 Ma

[29] Prior to extension, the northwestern Basin and Range witnessed long-lived, voluminous magmatism [Noble *et al.*, 1970; Lerch *et al.*, 2005a; Colgan *et al.*, 2006a]. The Black Rock, Pine Forest, and Warner Ranges (Figure 2) record basaltic through rhyolitic volcanism that dominated the landscape from the late Eocene to the Pliocene. As described above (Regional Geology and Geophysics), ~ 2 – 3 km of volcanic cover accumulated in the vicinity of the Warner Range, with slightly less (~ 1 – 2 km) deposited to the east near the Black Rock and Pine Forest Ranges.

[30] Because the volcanic products represent an interplay between magmatic addition to the crust and assimilation (partial-melting) of the country rock, we cannot simply remove the volcanic cover to arrive at an estimate of pre-volcanic crustal thickness. Volcanism across this region varied greatly in composition, and occurred in three main episodes that provided 1–3 km of volcanic cover since the late Eocene. Because isotope geochemistry has not been carefully studied for most of the Cenozoic volcanic units, estimating the ratio of crustal magmatic addition to erupted material is difficult. Through our velocity and amplitude modeling, we find only marginal evidence for mafic underplating ($V_p \sim 7.4$ km/s, thickness $\sim 1 \pm 1$ km) at the base of the crust (Figure 11), leaving no straightforward way to directly measure the amount of magmatic addition. Previous attempts to relate the degree of assimilation (crustal melting) to recharge (magmatic addition) have been made for the Basin and Range province [e.g., Perry *et al.*, 1993], but have not addressed our study area specifically. Although calculated assimilation/

recharge (a/r) ratios in the Basin and Range province vary over two orders of magnitude for different episodes of magmatism and different igneous compositions, observed patterns in magmatic characteristics narrow the likely range of this ratio. By simply taking an average of values through time, *Perry et al.* [1993] note that late Oligocene rhyolites have an a/r ranging from 0.75–3 (for simplicity we use the average of these two values, 1.9), whereas Miocene-Pliocene rhyolites display $a/r \leq 0.5$. In the case of the northwestern Basin and Range transition zone, we observe ≤ 1 km of Oligocene rhyolitic material, and ≤ 1 km of Miocene rhyolitic material [e.g., *Noble et al.*, 1970; *Duffield and McKee*, 1986; *Colgan et al.*, 2006a], providing an upper limit for the mantle contribution to these flows of ~ 1.0 km. This estimate does not account for mafic material added to the crust that cooled at depth, an inherently difficult quantity to constrain. In their tectonic and magmatic reconstruction of the eastern Basin and Range, *Gans et al.* [1989] assume that an amount of magma equal to or larger than the observed volcanic material intruded the crust but was not erupted. Recognizing the uncertainty in this step in our reconstruction, we estimate $\sim 2 \pm 1$ km of material may have been added to the crust related to the production of rhyolitic volcanism. The local thickness of basaltic products is generally no greater than 1 km, and in many places is significantly less (here we assume an average thickness of 0.5 km). Assimilation/recharge ratios for basalts are commonly lower than for rhyolites ($a/r \leq 0.3$ [e.g., *DePaolo*, 1985; *Stewart and DePaolo*, 1990]), providing a maximum estimate of the basalt-producing magmatic addition of ~ 0.4 km. Combining the upper estimates of magmatic addition since Eocene time, and applying a conservative uncertainty to our calculation, we arrive at a total of 2.4 ± 2 km. Because the uncertainty introduced in this phase of our reconstruction is uncorrelated with that from the restoration of Basin and Range extension, we take the RMS of the two steps thus far (restoring Basin and Range extension and removing latest Eocene to Miocene magmatism), reaching a total uncertainty of ± 2.25 km (Figure 12c).

[31] In the modern crustal section, we infer the existence of Sierra Nevada arc beneath the eastern Sheldon Plateau, Black Rock Range, and Jackson Mountains, marked by a low-velocity upper crust. Prior to Cenozoic Basin and Range magmatism, unmodified arc material may have extended through the entire crust (Figure 12c), providing a

crustal column more similar to that observed in the southern Sierra Nevada [*Fliedner et al.*, 2000].

5.3. Tectonic Reconstruction at 90 Ma

[32] The tectonic histories of the eastern and western portions of our study area differed sharply during the late Cretaceous to middle Cenozoic. As described in more detail above (Regional Geology and Geophysics), upper crustal (depth ≤ 5 km) granitic, metasedimentary, and metavolcanic lithologies [*Compton*, 1960] east of the Sheldon Plateau were exhumed from ~ 90 –60 Ma, and this region was characterized by subdued topography and minor sedimentation when volcanism began in the late Eocene [*Lerch et al.*, 2005a; *Colgan et al.*, 2006a]. To the west in the Warner Range, late Eocene andesites overlie a thick (>1.5 km) subaerial to submarine sedimentary section [*Duffield and McKee*, 1986; *Miller et al.*, 2005]. Granitic cobbles from a coarse conglomerate near the base of the Warner Range section yielded U-Pb zircon ages of ~ 113 and ~ 171 Ma [*Miller et al.*, 2005], common granitic crystallization ages in northwestern Nevada [e.g., *Wyld*, 1992; *Colgan et al.*, 2006b]. On the basis of these regional patterns, it is reasonable that much of the material removed from northwestern Nevada in the early Cenozoic was transported and deposited to the west in northern California and southern Oregon. By restoring the material associated with the unroofing of the upper crustal batholithic rocks in northwestern Nevada (4 ± 3 km), and removing the sedimentation from northeastern California (2 ± 1 km), we arrive at a sketch of crustal thickness across this region that is markedly different from today (Figure 12d). Thus, at ~ 90 Ma, the present-day Basin and Range transition zone was instead a transition from standard crustal thickness of ~ 40 km (global average ~ 41 km [*Christensen and Mooney*, 1995]) in the east, to thin (~ 34 km) continental-margin type crust in the west. This estimated crustal thickness under the western end of our survey is between the global averages for rifts and extended crust (~ 37 and ~ 31 km, respectively [*Christensen and Mooney*, 1995]), compatible with its depositional setting at late-Cretaceous to early-Tertiary time. Thus a westward-thinning continental margin at 90 Ma has evolved into an eastward-thinning rift shoulder at the present day. The transition between thicker and thinner crust occurred at the location of the then-waning Sierra Nevada magmatic arc, and it is possible that a deeper crustal root existed between thinner crust to both the west and east. However, because of the significant erosion

recorded inboard of the arc at this time, we speculate that arc thickness was ~ 40 km, transitional between the continental interior to the east and the continental margin to the west, and that no continuous high barrier separated these regions.

6. Conclusions

[33] In addition to broadly confirming the crustal thickness and velocity structure of previous geophysical studies from neighboring regions, our combined seismic and potential field data constrain the crustal response to magmatism and extension, and the Cretaceous-to-present tectonic evolution of this region.

[34] Basin and Range extension in this region has spanned the late Miocene to present and appears to have been relatively homogeneous with depth: we observe no evidence that deformation of the lower crust was significantly different in magnitude than the upper-crustal extension recorded at the surface. This statement is supported by the absence of distributed lower-crustal reflectivity, commonly attributed to large-magnitude ductile deformation, and by crustal thinning that is proportional to the amount of upper-crustal extension ($\sim 20\%$, Figure 7). Because we interpret there to have been no significant material transport away from this region during Basin and Range extension (e.g., lower-crustal flow in excess of the transport by extension), reconstructing the pre-extensional history produces only moderately thick crust (~ 40 km, on par with the global average for continental crust). Crustal thickness in northwestern Nevada, according to our reconstruction, appears to have never been as great as it is inferred to have been in the more highly extended portions of the Basin and Range where pre-extensional thicknesses are estimated to have been 45–55 km [e.g., *Smith et al.*, 1991], and where large crustal thicknesses may have helped trigger extension.

[35] The widespread magmatism that has occurred in this region over the last ~ 35 Ma undoubtedly altered the crustal composition through the addition of mantle-derived melts, evidenced by the large amount of basaltic material erupted over this time interval. Despite this long-lived magmatic activity, there appears to be no discrete high-velocity ($7.x$ km/s) zone in the lower crust equivalent to that claimed by *Catchings and Mooney* [1991] in the 1986 PASSCAL survey in northwestern Nevada (~ 130 km south of our experiment). We do not believe the lack of a lower-crustal $7.x$ layer

in our study area necessarily contradicts the *Catchings and Mooney* [1991] interpretation of the 1986 PASSCAL survey for two reasons: (1) the degree of lower-crustal extension under the northwestern end of the 1986 PASSCAL line is interpreted to be significantly greater on the basis of the presence of distributed lower-crustal reflectivity and may have enhanced the development of a $7.x$ layer in the PASSCAL survey area, and (2) our amplitude modeling indicates a gradient of high velocities near the Moho that may be produced by distributed mafic material.

[36] Our data document the location of the Cretaceous arc as it trends northeastward from the northern Sierra Nevada to southern Idaho, consistent with the surface exposures of Cretaceous granitic rocks (Figure 2) [*Barton et al.*, 1988]. The 1-D velocity profile of the low upper-crustal velocities near the Black Rock Range and Black Rock Desert is similar to that obtained from the southern Sierra Nevada to mid-crustal depths (Figure 10), and our gravity modeling supports the presence of granitic material by having a higher V_p/ρ ratio than the average of all basement lithologies [*Brocher*, 2005].

[37] Our estimated crustal thicknesses for the eastern and western ends of our survey at 90 Ma fit well with the late Cretaceous tectonic setting of this region. The thin crust (~ 34 km) under what is now northeastern California allowed for the accumulation of a thick late-Cretaceous to early-Tertiary sedimentary section. This sedimentary material appears to have been derived from northern Sierra Nevada arc and the relatively thicker crust (~ 40 km) to the east that underwent regional exhumation and unroofing in the late Cretaceous [*Miller et al.*, 2005; *Colgan et al.*, 2006a, 2006b].

Acknowledgments

[38] We would like to thank the hard-working volunteers who made this experiment possible: Tom Burdette, Ewenet Gashawbeza, Charlie Wilson, Adam Abeles, Martins Akintunde, Steve Azevedo, Lloyd Carothers, Matt Coble, Trevor Dumitru, Anne Egger, Julie Fosdick, Tyson Fulmer, Nathan Fung, Bob Greschke, Kelly Grijalva, Aaron Hirsch, Nick Hoffman, Julia James, Kyrill Krylov, Nick Leindecker, Mingjun Liu, Simone Manganelli, Chris Mattinson, Nic Markman, Darlene McEwan, Walter Mooney, Marleen Nyst, Willy Rittase, Brian Romans, Dave Scholl, Mario Torres, Amy Weislogel, and Charlie Wilson Sr. We thank E. Brueckl (Vienna Univ. of Technology), H. Thybo (Univ. of Copenhagen), P. Heikkinen (Univ. of Helsinki), A. Guterch (Polish Academy of Sciences), and C. Knapp (Univ. of South Carolina) for the use of their Texans. Farn-Yuh Menq and Cecil Hoffpauir operated the NEES-UT

Austin T-Rex vibrator. The Twin Creeks (Newmont Mining Corporation) and Florida Canyon (Apollo Gold Corporation) mines generously provided access to their properties and coordinated mine blasts with our recording windows. We also thank Colin Zelt, Barry Zelt, and Fujie Gou for making their velocity modeling software available. Andy Calvert, Bryan Kerr, and Eiji Kurashimo provided necessary guidance related to the velocity modeling. Conversations with George Thompson greatly strengthened our tectonic interpretations. Constructive reviews from Kate Miller and Randy Keller improved the clarity of this paper. Principal funding for explosive-source profiling was provided by NSF-Earthscope grant 0346245 and by the Petroleum Research Fund of the American Chemical Society; support for Vibroseis profiling was received from NSF-Geoenvironmental Engineering and Geohazard Mitigation grant 0444696; and funding for passive-source deployments came from Stanford University. Field support and instruments were provided to all parts of the experiment by the PASSCAL Instrument Center. All seismic data are available through the IRIS DMC.

References

- Allmendinger, R., T. Hauge, E. Hauser, C. Potter, S. Klemperer, K. Nelson, P. Kneupfer, and J. Oliver (1987), Overview of the COCORP 40°N transect, western United States: The fabric of an orogenic belt, *Geol. Soc. Am. Bull.*, *98*, 308–319.
- Barton, M., D. Battles, G. Debout, R. Capo, J. Christensen, S. Davis, R. Hanson, C. Michelsen, and H. Trim (1988), Mesozoic contact metamorphism in the western United States, in *Rubey Colloquium on Metamorphism and Crustal Evolution of the Western United States*, vol. 7, *Metamorphism and Crustal Evolution of the Western United States*, edited by W. Ernst, pp. 110–178, Univ. of Calif., Los Angeles.
- Beaudoin, B., et al. (1996), Transition from slab to slabless: Results from the 1993 Mendocino Triple Junction seismic experiment, *Geology*, *24*, 195–199.
- Best, M., and E. Christiansen (1991), Limited extension during peak Tertiary volcanism, Great Basin of Nevada and Utah, *J. Geophys. Res.*, *96*, 13,509–13,528.
- Best, M., E. Christiansen, A. Deino, C. Gromme, E. McKee, and D. Noble (1989), Eocene through Miocene volcanism in the Great Basin of the western United States, in *Field Excursions to Volcanic Terranes in the Western United States*, vol. II, *Cascades and Intermountain West*, Mem. N. M. Bur. Mines Miner. Resour., *47*, 91–133.
- Blackwell, D., J. Steele, and L. Carter (1991), Heat-flow patterns of the North American continent: A discussion of the geothermal map of North America, in *Decade of North American Geology*, vol. 1, Neotectonics of North America, edited by D. Slemmons et al., pp. 423–436, Geol. Soc. of Am., Boulder, Colo.
- Blakely, R. (1995), *Potential Theory in Gravity and Magnetic Applications*, Cambridge Univ. Press, New York.
- Blakely, R., and G. Connard (1989), Crustal studies using magnetic data, in *Geophysical Framework of the Continental United States*, edited by L. Pakiser and W. Mooney, Mem. Geol. Soc. Am., *172*, 45–60.
- Blakely, R., and R. Jachens (1991), Regional study of mineral resources in Nevada: Insights from three-dimensional analysis of gravity and magnetic anomalies, *Geol. Soc. Am. Bull.*, *103*, 795–803.
- Block, L., and L. Royden (1990), Core complex geometries and regional scale flow in the lower crust, *Tectonics*, *9*, 557–567.
- Brocher, T. (2005), Empirical relations between elastic wave-speeds and density in the Earth's crust, *Bull. Seismol. Soc. Am.*, *95*, 2081–2092.
- Carmichael, I., R. Lange, C. Hall, and P. Renne (2006), Faulted and tilted Pliocene olivine-tholeiite lavas near Alturas, NE California, and their bearing on the uplift of the Warner Range, *Geol. Soc. Am. Bull.*, *118*, 1196–1211.
- Catchings, R. (1992), A relation among geology, tectonics, and velocity structure, western to central Nevada Basin and Range, *Geol. Soc. Am. Bull.*, *104*, 1178–1192.
- Catchings, R., and W. Mooney (1991), Basin and Range crustal and upper mantle structure, northwest to central Nevada, *J. Geophys. Res.*, *96*, 6247–6267.
- Chapman, R., and C. Bishop (1968), Bouguer gravity map of California, Alturas Sheet, scale 1:250,000, Calif. Div. of Mines and Geol., Sacramento.
- Christensen, N., and W. Mooney (1995), Seismic velocity structure and composition of the continental crust: A global view, *J. Geophys. Res.*, *100*, 9761–9788.
- Christiansen, R., R. Yeats, S. Graham, W. Niem, A. Niem, and P. Snively (1992), Post-Laramide geology of the U.S. Cordilleran region, in *The Geology of North America*, vol. G2, *The Cordilleran Orogen: Conterminous U. S.*, edited by B. Burchfiel, P. W. Lipman, and M. L. Sack, pp. 261–406, Geol. Soc. of Am., Boulder, Colo.
- Colgan, J., T. Dumitru, and E. Miller (2004), Diachroneity of Basin and Range extension and Yellowstone hotspot volcanism in northwestern Nevada, *Geology*, *32*, 121–124.
- Colgan, J., T. Dumitru, M. McWilliams, and E. Miller (2006a), Timing of Cenozoic volcanism and Basin and Range extension in northwestern Nevada: New constraints from the northern Pine Forest Range, *Geol. Soc. Am. Bull.*, *118*, 126–139.
- Colgan, J., T. Dumitru, E. Miller, and P. Reiners (2006b), Cenozoic tectonic evolution of the Basin and Range Province in northwestern Nevada, *Am. J. Sci.*, *306*, 616–654.
- Compton, R. (1960), Contact metamorphism in the Santa Rosa Range, Nevada, *Geol. Soc. Am. Bull.*, *71*, 1383–1416.
- DePaolo, D. (1985), Isotopic studies of processes in mafic magma chambers: I. The Kiglapait Intrusion, Labrador, *J. Petrol.*, *26*, 925–951.
- Duffield, W., and E. McKee (1986), Geochronology, structure, and basin-range tectonism of the Warner Range, northeastern California, *Geol. Soc. Am. Bull.*, *97*, 142–146.
- Emmons, W. (1907), Normal faulting in the Bullfrog District, Nevada, *Science*, *26*, 221–222.
- Ernst, W. (1999), Mesozoic petroTECTONIC development of the Sawyers Bar suprasubduction-zone arc, central Klamath Mountains, northern California, *Geol. Soc. Am. Bull.*, *111*, 1217–1232.
- Fliedner, M., S. Klemperer, and N. Christensen (2000), Three-dimensional seismic model of the Sierra Nevada Arc, California, and its implications for crustal and upper mantle composition, *J. Geophys. Res.*, *105*, 10,899–10,921.
- Fosdick, J., A. Egger, J. Colgan, B. Surpless, E. Miller, and D. Lerch (2005), Cenozoic evolution of the northwestern boundary of the Basin and Range: Geologic constraints from the Warner Range and Surprise Valley region, *Geol. Soc. Am. Abstr. Programs*, *37*, 70.
- Gans, P. (1988), An open-system, two-layer crustal stretching model for the eastern Great Basin, *Tectonics*, *6*, 1–12.

- Gans, P., G. Mahood, and E. Schermer (1989), Synextensional magmatism in the Basin and Range Province: A case study from the eastern Great Basin, *Geol. Soc. Am. Spec. Pap.*, 233.
- Gashawbeza, E., D. Lerch, C. Wilson, S. Klemperer, and E. Miller (2005), Integrated passive and active source seismic investigation of the northwestern Basin and Range Province, *Eos Trans. AGU*, 86(52), Fall Meet. Suppl., Abstract S41A-0973.
- Gilbert, H. J., and A. F. Sheehan (2004), Images of crustal variations in the intermountain west, *J. Geophys. Res.*, 109, B03306, doi:10.1029/2003JB002730.
- Girty, G., R. Hanson, M. Girty, R. Schweickert, D. Harwood, A. Yoshinobu, K. Bryan, J. Skinner, and C. Hill (1995), Timing of emplacement of the Haypress Creek and Emigrant Gap plutons: Implications for the timing and controls of Jurassic orogenesis, northern Sierra Nevada, California, in *Jurassic Magmatism and Tectonics of the North American Cordillera*, edited by D. Miller and C. Busby, *Geol. Soc. Am. Spec. Pap.*, 299, 191–202.
- Glen, J., D. Lerch, S. Klemperer, and D. Ponce (2005), Seismic refraction and potential field modeling from the northwestern Basin and Range transition zone, Nevada and California, *Eos Trans. AGU*, 86(52), Fall Meet. Suppl., Abstract T51D-1367.
- Hill, D., and L. Pakiser (1976), Seismic-refraction study of crustal structure between the Nevada Test Site and Boise, Idaho, *Geol. Soc. Am. Bull.*, 78, 685–704.
- Holbrook, W. (1990), The crustal structure of the northwest Basin and Range Province, Nevada, *J. Geophys. Res.*, 95, 21,843–21,869.
- Holbrook, W., R. Catchings, and C. Jarchow (1991), Origin of deep crustal reflections: Implications of coincident seismic refraction and reflection data in Nevada, *Geology*, 19, 175–179.
- Irwin, W. (2003), Correlation of the Klamath Mountains and Sierra Nevada, *U.S. Geol. Surv. Open File Rep.*, OF02-0490.
- Irwin, W., and J. Wooden (2001), Map showing plutons and accreted terranes of the Sierra Nevada, California with a tabulation of U/Pb isotopic ages, *U.S. Geol. Surv. Open File Rep.*, OF01-0229.
- Jarchow, C., G. Thompson, R. Catchings, and W. Mooney (1993), Seismic evidence for active magmatic underplating beneath the Basin and Range Province, western United States, *J. Geophys. Res.*, 98, 22,095–22,108.
- Jennings, C., R. Strand, and T. Rogers (1977), Geologic map of California, scale 1:750,000, Calif. Div. of Mines and Geol., Sacramento.
- Klemperer, S., T. Hauge, E. Hauser, J. Oliver, and C. Potter (1986), The Moho in the northern Basin and Range Province, Nevada, along the COCORP 40°N seismic reflection transect, *Geol. Soc. Am. Bull.*, 97, 603–618.
- Lerch, D., J. Colgan, E. Miller, and M. McWilliams (2005a), Tectonic and magmatic evolution of the northwestern Basin and Range transition zone: Mapping and geochronology from the Black Rock Range, NV, *Geol. Soc. Am. Abstr. Programs*, 37, 70.
- Lerch, D., S. Klemperer, K. Stokoe, and F. Menq (2005b), Application of the NEES T-Rex vibrator for 3-component crustal reflection/refraction profiling: 2004 test in the Basin and Range, *Eos Trans. AGU*, 86(52), Fall Meet. Suppl., Abstract S23B-0258.
- Louie, J., W. Thelen, S. Smith, J. Scott, M. Clark, and S. Pullammanappallil (2004), The northern Walker Lane refraction experiment: P_n arrivals and the northern Sierra Nevada root, *Tectonophysics*, 388, 253–269.
- Ludwig, W., J. Nafe, and C. Drake (1970), Seismic refraction, in *The Sea*, vol. 4, edited by A. Maxwell, pp. 53–84, John Wiley, Hoboken, N. J.
- McKee, E. (1971), Tertiary igneous chronology of the Great Basin of the western United States: Implications for tectonic models, *Geol. Soc. Am. Bull.*, 82, 3497–3501.
- McKenzie, D., F. Nimmo, J. Jackson, P. Gans, and E. Miller (2000), Characteristics and consequences of flow in the lower crust, *J. Geophys. Res.*, 105, 11,029–11,046.
- McKnight, B. (1984), Stratigraphy and sedimentology of the Payne Cliffs Formation, southwestern Oregon, in *Oregon and California, Field Trip Guidebook—Pacific Section*, vol. 42, *Geology of the Upper Cretaceous Hornbrook Formation*, edited by T. Nilsen, pp. 187–194, Soc. of Econ. Paleontol. and Mineral., Tulsa, Okla.
- Miller, E., M. Miller, J. Wright, and R. Madrid (1992), Late Paleozoic paleogeographic and tectonic evolution of the western U. S. Cordillera, in *Decade of North American Geology*, vol. 1, Neotectonics of North America, edited by D. Slemmons et al., pp. 57–106, Geol. Soc. of Am., Boulder, Colo.
- Miller, E., T. Dumitru, R. Brown, and P. Gans (1999), Rapid Miocene slip on the Snake Range–Deep Creek Range fault system, east-central Nevada, *Geol. Soc. Am. Bull.*, 111, 886–905.
- Miller, E., J. Colgan, B. Surpless, S. Riedel, A. Strickland, A. Egger, and D. Benoit (2005), Drill core data from the Warner Range and Surprise Valley, *Geol. Soc. Am. Abstr. Programs*, 37, 203–204.
- Mooney, W., and C. Weaver (1989), Regional crustal structure and tectonics of the Pacific coastal states: California, Oregon, and Washington, in *Geophysical Framework of the Continental United States*, edited by L. Pakiser and W. Mooney, *Mem. Geol. Soc. Am.*, 172, 129–161.
- Morgan, P., and W. Gosnold (1989), Heat flow and thermal regimes in the continental United States, in *Geophysical Framework of the Continental United States*, edited by L. Pakiser and W. Mooney, *Mem. Geol. Soc. Am.*, 172, 493–522.
- Nilsen, T. (1993), Stratigraphy of the Cretaceous Hornbrook Formation, southern Oregon and northern California, *U. S. Geol. Surv. Prof. Pap.*, P1521.
- Noble, D., E. McKee, J. Smith, and M. Korringa (1970), Stratigraphy and geochronology of Miocene volcanic rocks in northwestern Nevada, *U.S. Geol. Surv. Prof. Pap.*, P0700-D, D23–D32.
- Parsons, T., G. Thompson, and N. Sleep (1994), Mantle plume influence on the Neogene uplift and extension of the U.S. western Cordillera?, *Geology*, 22, 83–86.
- Perry, F., D. DePaolo, and W. Baldrige (1993), Neodymium isotopic evidence for decreasing crustal contributions to Cenozoic ignimbrites of the western United States: Implications for the thermal evolution of the Cordilleran crust, *Geol. Soc. Am. Bull.*, 105, 872–882.
- Pierce, L., and K. Morgan (1992), The track of the Yellowstone hot spot: Volcanism, faulting, and uplift, in *Regional Geology of Eastern Idaho and Western Wyoming*, edited by P. Link, M. Kuntz, and L. Platt, *Mem. Geol. Soc. Am.*, 179, 1–53.
- Plouff, D. (1985), Many gravity lows may reflect Cenozoic plutons beneath volcanic terranes of the western United States, *Eos Trans. AGU*, 66, 845.
- Plouff, D. (1997), Resource assessment of the Bureau of Land Management's Winnemucca District and Surprise Resource Area, northwest Nevada and northeast California, *U.S. Geol. Surv. Open File Rep.*, OF97-99.

- Ponce, D. A. (1997), Gravity map of Nevada, *U.S. Geol. Surv. Digital Data Ser., DDS-42*.
- Quinn, M., J. Wright, and S. Wyld (1997), Happy Creek igneous complex and tectonic evolution of the early Mesozoic arc in the Jackson Mountains, northwest Nevada, *Geol. Soc. Am. Bull.*, *109*, 461–482.
- Seedorff, E. (1991), Magmatism, extension, and ore deposits of Eocene to Holocene age in the Great Basin: Mutual effects and preliminary proposed genetic relationships, in *Geology and Ore Deposits of the Great Basin*, edited by G. Raines et al., pp. 133–178, Geol. Soc. of Nev., Reno.
- Smith, D., P. Gans, and E. Miller (1991), Palinspastic restoration of Cenozoic extension in the central and eastern Basin and Range Province at latitude 39–40°N, in *Geology and Ore Deposits of the Great Basin*, edited by G. Raines et al., pp. 75–86, Geol. Soc. of Nev., Reno.
- Smith, R., L. Braile, J. Steidtmann, and S. Roberts (1993), Topographical signature, space-time evolution, and physical properties of the Yellowstone–Snake River plain volcanic system: The Yellowstone hotspot, in *Geology of Wyoming, Mem.*, vol. 5, edited by A. Snoke, J. Steidtmann, and S. Roberts, pp. 694–754, Geol. Surv. of Wyo., Laramie.
- Snyder, D., C. Roberts, R. Saltus, and R. Sikora (1981), Magnetic tape containing the principal facts of 64402 gravity stations in the state of California, *Rep. PB82-168287*, U.S. Geol. Surv., Reston, Va.
- Stewart, B., and D. DePaolo (1990), Isotopic studies of processes in mafic magma chambers: II. The Skaergaard Intrusion, east Greenland, *J. Petrol.*, *104*, 125–141.
- Stewart, J., and J. Carlson (1978), Geologic map of Nevada, scale 1:500,000, U.S. Geol. Surv., Reston, Va.
- Stockli, D. (1999), Regional timing and spatial distribution of Miocene extension in the northern Basin and Range Province, Ph.D. thesis, Stanford Univ., Stanford, Calif.
- Stoerzel, A., and S. Smithson (1998), Two-dimensional travel time inversion for crustal P and S wave velocity structure of the Ruby Mountains metamorphic core complex, NE Nevada, *J. Geophys. Res.*, *103*, 21,121–21,143.
- Surpluss, B. E., D. F. Stockli, A. Trevor Dumitru, and E. L. Miller (2002), Two-phase westward encroachment of Basin and Range extension into the northern Sierra Nevada, *Tectonics*, *21*(1), 1002, doi:10.1029/2000TC001257.
- Talwani, M., J. Worzel, and M. Landisman (1959), Rapid gravity computations for two-dimensional bodies with application to the Mendocino submarine fracture zone, Pacific Ocean, *J. Geophys. Res.*, *64*, 49–59.
- Trehu, A., I. Asudeh, T. Brocher, J. Luetgert, W. Mooney, J. Nabelek, and Y. Nakamura (1994), Crustal structure of the Cascadia Forearc, *Science*, *266*, 237–243.
- Walker, G., and N. MacLeod (1991), Geologic map of Oregon, scale 1:500,000, U.S. Geol. Surv., Reston, Va.
- Wernicke, B. (1992), Cenozoic extensional tectonics of the U.S. Cordillera, in *Decade of North American Geology*, vol. 1, Neotectonics of North America, edited by D. Slemmons et al., pp. 553–581, Geol. Soc. of Am., Boulder, Colo.
- Wyld, S. (1992), Geology and geochronology of the Pine Forest Range, northwest Nevada: Stratigraphic, structural and magmatic history, and regional implications, Ph.D. thesis, Stanford Univ., Stanford, Calif.
- Wyld, S. (1996), Early Jurassic deformation in the Pine Forest Range, northwest Nevada, and implications for Cordilleran tectonics, *Tectonics*, *15*, 566–583.
- Wyld, S. (2000), Triassic evolution of the arc and backarc of northwestern Nevada, and evidence for extensional tectonism, in *Paleozoic and Triassic Paleogeography and Tectonics of Western Nevada and Northern California*, edited by M. Soreghan and G. Gehrels, *Spec. Pap. Geol. Soc. Am.*, *347*, 185–207.
- Wyld, S. (2002), Structural evolution of a Mesozoic backarc fold-and-thrust belt in the U. S. Cordillera: New evidence from northern Nevada, *Geol. Soc. Am. Bull.*, *114*, 1452–1468.
- Wyld, S., and J. Wright (2001), New evidence for Cretaceous strike-slip faulting in the United States Cordillera and implications for terrane-displacement, deformation patterns, and plutonism, *Am. J. Sci.*, *301*, 150–181.
- Zelt, B., R. Ellis, and R. Clowes (1993), Crustal structure in the eastern Insular and southernmost Coast belts, Canadian Cordillera, *Can. J. Earth Sci.*, *30*, 1014–1027.
- Zelt, C., and R. Smith (1992), Seismic traveltimes inversion for 2-D crustal velocity structure, *Geophys. J. Int.*, *108*, 16–34.
- Zoback, M., and G. Thompson (1978), Basin and Range rifting in northern Nevada: Clues from a mid-Miocene rift and its subsequent offsets, *Geology*, *6*, 111–116.
- Zoback, M., E. McKee, R. Blakely, and G. Thompson (1994), The northern Nevada rift: Regional tectono-magmatic relations and middle Miocene stress direction, *Geol. Soc. Am. Bull.*, *106*, 371–382.
- Zucca, J., G. Fuis, B. Milkereit, W. Mooney, and R. Catchings (1986), Crustal structure of northeastern California, *J. Geophys. Res.*, *91*, 7359–7382.